pK_a and Aggregation of Bilirubin: Titrimetric and Ultracentrifugation Studies on Water-Soluble Pegylated Conjugates of Bilirubin and Fatty Acids†

Stefan E. Boiadjiev,‡ Kimberly Watters,‡ Steven Wolf,‡ Bryon N. Lai,‡ William H. Welch,⊥ Antony F. McDonagh,*,§ and David A. Lightner*,‡,⊥

Departments of Chemistry and Biochemistry, University of Nevada, Reno, Nevada 89557-0020, and Division of Gastroenterology and The Liver Center, University of California, San Francisco, California 94143-0538

Received August 26, 2004; Revised Manuscript Received September 17, 2004

ABSTRACT: A water-soluble conjugate (**1**) with intact carboxyl groups was prepared by addition of poly(ethylene glycol) thiol (MPEG-SH) regiospecifically to the *exo* vinyl group of bilirubin. ^{1}H and ^{13}C NMR and absorbance spectroscopy in $CDCl_3$ and DMSO-d_6 confirmed the assigned structure and showed that pegylation did not disrupt the hydrogen-bonded ridge-tile conformation of the pigment moiety. Aqueous solutions of **1** were optically clear, but NMR signals were seen only from the MPEG portion and none from the tetrapyrrole, consistent with dissolved assemblies containing aggregated bilirubin cores within mobile polyether chains. On alkalinization (pH >12), signals from the pigment moiety reappeared. Titrimetric measurements on **1** in water showed the pK_a's of the two carboxyl groups to be similar (average 6.42). Control studies with pegylated half-esters of succinic, suberic, brassylic, thapsic, and 1,20-eicosanedioic acid showed that pegylation per se has little, if any, effect on carboxyl ionization. However, aggregation increases the apparent pK_a by ∼1−2 units. The molecularity of bilirubin in solution was further characterized by ultracentrifugation. Over the pH range 8.5−10 in buffer, bilirubin formed multimers with aggregation numbers ranging from ∼2−7. Bilirubin is monomeric in DMSO or $CHCl_3$ at $\sim 2 \times 10^{-5}$ M, but aggregation occurred when the $CHCl_3$ was contaminated with trace adventitious (perhaps lipoidal) impurities. These observations show that aggregation increases the pK_a's of aliphatic carboxylic acids relative to their monomer values in water. They are consistent with earlier ^{13}C NMR-based estimates of ∼4.2 and ∼4.9 for the aqueous pK_a's of bilirubin and similar studies of bilirubin in micellar bile-salt solutions. Together with earlier work, they confirm that the pK_a's of bilirubin are about normal for aliphatic carboxyls and suggest that the high (>7.5) values occasionally reported, including those based on $CHCl_3$ partitioning, are artifacts of aggregation or technique.

Bilirubin, a tetrapyrrolic dicarboxylic acid (Figure 1), is the cytotoxic yellow pigment of jaundice (*1*). Produced in healthy adults at about 300 mg/day by catabolism of heme, it is eliminated by the following series of poorly understood steps: delivery to the liver as a complex with serum albumin (SA);[1] dissociation from SA and uptake by hepatocytes; migration within hepatocytes to the endoplasmic reticulum where it is converted to mono- and diglucuronides by a bilirubin-specific glucuronosyl transferase (UGT1A1); passage of the glucuronides to the apical (canalicular) membrane; efflux of the glucuronides, but not the parent unconjugated pigment, into bile by the organic anion ABC transporter MRP2 (*2*). Even less well understood than these processes are the mechanisms of uptake of bilirubin into the brain and its neurological toxicity. Nevertheless, bilirubin has proved an informative model for the metabolism and transport of many xenobiotic carboxylic cholephilic organic anions, and considerable interest in the pigment has been rekindled recently by the rediscovery of its potent antioxidant properties and mounting evidence that it is a major physiologic cytoprotectant (*3*, *4*).

The structure, state of aggregation, and degree of ionization of bilirubin in vivo are clearly key determinants of its biochemical properties. Although bilirubins's chemical structure is frequently misrepresented or misinterpreted (*5*), its constitution and structure in the solid state and in solution in organic solvents are well-established. Its aggregation, which may be involved in its neurotoxicity and is a common, often overlooked, source of difficulty and error in experimental work (*6*), is less well characterized. And, although the two acidic side chains in bilirubin are simple aliphatic

† This work was supported by National Institutes of Health Grants HD-17779, DK-26307, and P30 DK-26743. Purchase of the ultracentrifuge was supported by an NSF/RIAS grant.

* To whom correspondence should be addressed. (AFMcD) Telephone: (415)476-6425. Fax: (415)476−0659. E-mail: tonymcd@itsa.ucsf.edu. (DAL) Telephone: (775) 784-4980. Fax: (775) 784−6804. E-mail: lightner@scs.unr.edu.

‡ Department of Chemistry, University of Nevada, Reno.

⊥ Department of Biochemistry, University of Nevada, Reno.

§ Division of Gastroenterology and The Liver Center, University of California, San Francisco.

[1] Abbreviations: ABC, ATP binding cassette; CTAB, cetyltrimethylammonium bromide; DMF, dimethyl formamide; DMSO, dimethyl sulfoxide; EPPS, 4-(2-hydroxyethyl)piperazine-1-propanesulfonic acid buffer; gHMBC, gradient heteronuclear multiple bond coherence; MPEG-OH (-SH, -OTs), poly(ethylene glycol) (thiol, tosylate) monomethyl ether; MRP2, multidrug resistance associated protein 2; NMR, nuclear magnetic resonance; PBLG, poly(γ-benzyl L-glutamate); PEG, poly(ethylene glycol); PEO, poly(ethylene oxide); SA, serum albumin; SDS, sodium dodecyl sulfate; UGT1A1, uridinediphosphoglucuronosyltransferase 1A1.

10.1021/bi0481491 CCC: $27.50
Published on Web 11/18/2004

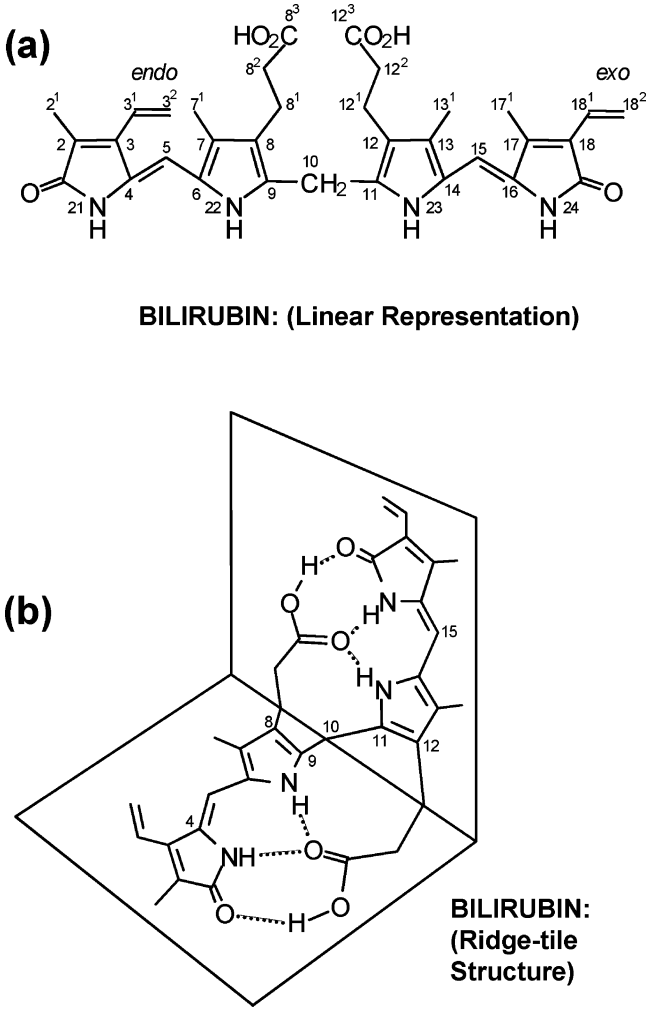

FIGURE 1: Bilirubin structure: (a) linear representation with conventional numbering system; (b) energetically most stable intramolecularly hydrogen-bonded structure shaped like a ridge-tile. Only one of two non-superimposable mirror-image ridge-tile conformations is shown.

carboxyl groups, accurate determination of their acidity constants (K_a's) in water has proved difficult because bilirubin is so insoluble at physiologic pH. While K_a's of $\sim 10^{-5}$ M (p$K_a \approx 5$) would be expected (*7*) and have been found in several experimental studies (*8*−*11*), values as low as 10^{-8}−10^{-10} M (pK_a 8−10) have also been reported (*12*−*14*) and used in efforts to explain bilirubin metabolism (*15*). No chemically credible explanation for such unprecedented low values has yet been advanced.

In 1995, Nogales and Lightner reported that the nuclear magnetic resonance (NMR) ^{13}C signal of the ^{13}COOH groups in the tetra-*n*-butylammonium salt of ^{13}C-enriched mesobilirubin XIIIα, a close bilirubin analogue, is essentially the same in H_2O/10% D_2O at pH 8.0 or pH 11.0 (δ 182.5 versus 182.4) *in the absence of any cosolvent such as dimethyl sulfoxide* (DMSO) (*16*). Since ^{13}C NMR signals of carboxylic acids are highly sensitive to ionization (e.g., δ 181.5 for acetate ion versus 176.8 for acetic acid) and ^{13}C chemical shifts can be measured with great accuracy and precision (*17*), this observation provided strong evidence that pK_a values of >8 for one or both of the COOH groups of bilirubin (*12*−*14*) could not be correct. This key finding led us to use a straightforward, sensitive, and well-validated ^{13}C NMR technique (*17*−*19*) to measure the pK_a's of 99% ^{13}C-labeled mesobilirubin XIIIα and mesobiliverdin XIIIα (*11*, *20*), synthetic pigments related very closely to natural bilirubin and biliverdin. Consistent with observations on the tetra-*n*-butylammonium salt and the conclusions of several earlier investigators (*8*−*10*, *21*) we found values for their COOH dissociation constants within the expected normal range. In those studies, we used up to 31 mol % DMSO as cosolvent to solubilize the pigments and validated the method using a large variety of mono-, di-, and tetrapyrrolic carboxylic acids as well as standards of known pK_a's (*11*, *20*, *22*). However, those studies, and those of earlier investigators (*8*, *10*), have been pooh-poohed because of the use of DMSO or dimethyl formamide (DMF) as (co)solvent (*23*) and the results attributed to artifacts of aggregation (*24*). Meanwhile, values of $pK_{a_1} = 8.2$ and $pK_{a_2} = 8.8$ continue to be invoked in the literature (*24*−*26*).

We now describe studies on the solution structure and acid dissociation constants of a water-soluble derivative of bilirubin (**1**) bearing a poly(ethylene glycol) (PEG) side chain

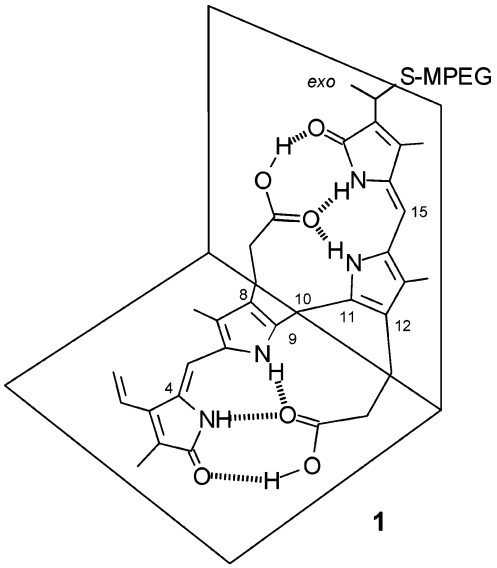

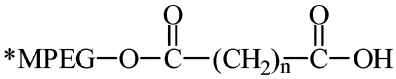

2: (n = 2) succinic
3: (n = 6) suberic
4: (n = 11) brassylic
5: (n = 14) thapsic
6: (n = 18) eicosanedioic

*MPEG-OH = Polyethyleneglycol monomethyl ether mol. wt ~ 1900

(*27*) and of a series of fatty-acid model compounds (**2**−**6**) solubilized in a similar way. These compounds dissolve readily in water without the need for a cosolvent such as DMSO, and their pK_a's can be readily measured titrimetrically. In complementary studies, we used ultracentrifugation to investigate the aggregation of bilirubin in organic solvents and aqueous buffers. The results provide firm experimental support for the validity of earlier NMR measurements (*8*, *11*, *20*, *21*) and reveal the marked influence of aggregation on the acid dissociation of bilirubin.

EXPERIMENTAL PROCEDURES

NMR measurements were done with a Varian Unity Plus spectrometer (11.75 T magnetic field strength; ^{1}H frequency 500 MHz; ^{13}C frequency 125 MHz) on solutions in $CDCl_3$ (referenced at 7.26 ppm for ^{1}H and 77.0 ppm for ^{13}C), $(CD_3)_2SO$ (referenced at 2.49 ppm for ^{1}H and 39.5 ppm for ^{13}C), or D_2O (referenced to external $CDCl_3$). *J*-modulated spin−echo (attached proton test) and gHMBC experiments were used to assign ^{13}C NMR signals. The carbon NMR spectra acquisition time was 15−16 h. UV−visible spectra were recorded on a Perkin-Elmer Lambda 12 spectrophotometer. Analytical ultracentrifugation was performed on a Beckman model E fitted with absorption scanning optics and a home-built computer interface. Radial chromatography was on a Chromatotron (Harrison Research, Inc., Palo Alto, CA) with 1, 2, or 4 mm thick rotors coated with Merck silica gel PF_{254} with $CaSO_4$ binder, preparative layer grade. Chloroform and DMSO used in ultracentrifugation and UV−visible spectroscopic experiments were Fisher HPLC grade. Deuterated solvents for NMR experiments were from Cambridge Isotope Labs; other spectral grade solvents were from Fisher-Acros. Deuterated chloroform was passed through a short column of Woelm alumina for chromatography (Super 1 activity) to remove acidic and polar impurities and used immediately. Bilirubin (Sigma) was purified, crystallized (*28*), and dried under vacuum (<1 mmHg) at ∼63 °C and found to contain less than 3% of the IIIα and XIIIα isomers; similar preparations reproducibly gave satisfactory C, H, N elemental combustion analyses for $C_{33}H_{36}N_4O_6$. Poly(ethylene glycol) monomethyl ether (MPEG-OH; average molecular weight 1900, ∼42 monomeric units), 3-hydroxybenzoic acid, succinic anhydride, suberic (1,8-octanedioic), brassylic (1,13-tridecanedioic), and thapsic (1,16-hexadecanedioic) acids were from Aldrich; 1,20-eicosanedioic acid was from TCI America Chemicals.

*MPEG-S−Bilirubin (**1**).* MPEG-S−bilirubin (**1**) was prepared according to Fontich et al. (*27*), by synthesis and addition of MPEG-SH to the *exo*-vinyl group of bilirubin. Thus, MPEG-OH was converted to its *p*-toluenesulfonate ester MPEG-OTs (*29*) in 89% yield by reaction with freshly purified *p*-toluenesulfonyl chloride in dichloromethane in the presence of triethylamine. (The tosylate is moderately stable upon storage if pyridine is not used as base.) MPEG-OTs was converted to MPEG-SH by treatment with aqueous thiourea followed by reflux with NaOH (*30*). Precautions were taken to keep the reaction mixture and workup under a nitrogen blanket at all times to prevent disulfide formation. An 85% yield of MPEG-SH with some disulfide was obtained. (The mercaptan is prone to air oxidation to the disulfide even in the solid state; thus, use of freshly prepared MPEG-SH is recommended.) According to Monti and Manitto (*31*), MPEG-SH can be expected to undergo Markovnikov addition to the *exo*-vinyl group of (a 1.2 mol excess of) bilirubin to afford adduct **1**. In a typical reaction, a mixture of 117 mg (0.2 mmol) of bilirubin, 340 mg (0.17 mmol) of MPEG-SH (freshly prepared), and 50 mL of dry $CHCl_3$ was purged with N_2 at 0 °C for 45 min. *p*-Toluenesulfonic acid (3 mg) was added, and the mixture was stirred in the dark for 24 h under N_2. It was diluted with CH_2Cl_2 (100 mL), and the organic phase was washed with saturated aqueous NH_4Cl (15 mL) and then H_2O (15 mL), dried over anhydrous $MgSO_4$, filtered, and evaporated under vacuum. Unreacted bilirubin was effectively removed by radial chromatography on silica gel, eluting with 1.5 vol % CH_3OH in CH_2Cl_2. A more polar yellow band was then eluted with 6.0−8.5 vol % CH_3OH in CH_2Cl_2. This, after evaporation to dryness, was taken up into dichloromethane as a concentrated solution and precipitated by a large volume of dry diethyl ether (peroxide-free) to afford, as bright yellow globular solid particles, 291 mg (58%) of covalently bound mixed polymer MPEG-S−bilirubin (**1**). This was immediately dried under vacuum over P_2O_5 and stored under nitrogen in the dark. ^{1}H NMR and ^{13}C NMR spectra were run on completely transparent, mobile solutions of **1** (38 mg samples, $\sim 1.5 \times 10^{-2}$ M) in $CDCl_3$ and $(CD_3)_2SO$, solvents in which **1** is freely soluble. Similarly, a 38 mg sample readily dissolved in distilled water (pH 7). The aqueous solution was somewhat viscous compared to the organic NMR solutions but still completely transparent. NMR studies were also run on aqueous solutions of **1** in D_2O−NaOD (pD > 12), D_2O followed by sonication for 75 min, D_2O/$(CD_3)_2SO$ (9:1, vol/vol), and D_2O/$(CD_3)_2SO$ (1:1, vol/vol).

As a control, a mechanical mixture of bilirubin + MPEG-SH was prepared from a clear, argon-purged solution of 58.5 mg (0.1 mmol) of bilirubin and 193 mg (0.1 mmol) of MPEG-SH (+ MPEG-S−S-MPEG) in 70 mL of $CHCl_3$, which was stirred for 15 min then evaporated to dryness. The residue was redissolved in a minimum volume of dry CH_2Cl_2 (∼10 mL), and this solution was added to 100 mL of dry diethyl ether at 0 °C. Precipitated solid was collected by filtration to afford a bright orange solid.

Fatty Acid MPEG Monoesters. Dicarboxylic acid MPEG-OH monoesters (**3**−**6**) were prepared by conversion of suberic (C_8), brassylic (C_{13}), thapsic (C_{16}), and eicosanedioic (C_{20}) acid to their diacid chlorides, followed by reaction with 0.8 equiv of MPEG-OH and purification by repeated precipitations from CH_2Cl_2 with dry diethyl ether. Products were characterized by ^{13}C and ^{1}H NMR (see below). For example, for the preparation of suberic acid MPG monoester **3**, a mixture of 436 mg (2.5 mmol) of suberic acid and 15 mL of freshly distilled thionyl chloride ($SOCl_2$) was heated at reflux under N_2 for 1.5 h. The mixture was cooled, excess of $SOCl_2$ was removed under vacuum, and residual $SOCl_2$ was chased out by coevaporation with anhydrous benzene (2 × 10 mL). The residue was dissolved in 10 mL of anhydrous CH_2Cl_2, and this solution was added to a precooled (ice bath) solution of 3.80 g (2 mmol) of MPEG-OH in 20 mL of CH_2Cl_2 containing 1.4 mL (10 mmol) of triethylamine and 2 mg of 4-(dimethylamino)pyridine. The ice bath was removed, and the mixture was stirred at ambient temperature for 3 h, then filtered. Water (0.5 mL) was added to the filtrate, and the mixture was evaporated under vacuum. The residue was redissolved in benzene (*TOXIC!*), and trifluoroacetic acid was added until a sample on wetted pH paper showed a pH just <7. Solvent was removed under vacuum, and the residue was precipitated three times by adding its solution in 20 mL of CH_2Cl_2 to 150 mL of cold anhydrous diethyl ether. The product was separated by filtration and dried under vacuum (0.5 mmHg) for 24 h. The product (3.91 g) showed a ^{1}H NMR ($CDCl_3$) signal for a free acid proton at 11.9 ppm and two ^{13}C carbonyl carbons at 173.3 and 175.1 ppm, respectively, for the ester and acid groups.

The MPEG monoester (**2**) of succinic acid (C_4) was prepared by heating MPEG-OH with succinic anhydride at 150 °C, according to Zalipsky et al. (*32*). The product was purified by triple reprecipitation from CH_2Cl_2 with dry diethyl ether to remove excess succinic anhydride.

Titrations. Potentiometric titrations of **1**−**6** were done in glass-distilled water at 23 °C with pH measured by an Orion model 811 pH/mV meter equipped with an Orion model 91-02 pH electrode with Ag/AgCl internal reference system and Orion ATC probe and buret delivery of 0.005−0.01 M sodium hydroxide solution that was standardized before each titration using potassium acid phthalate primary standard. The method was calibrated by titration of aqueous propionic acid. For **1**, four separate solutions (∼504 mg in 25 mL of doubly distilled water) were titrated under dimmed light with magnetic stirring with 1.06×10^{-2} M aqueous NaOH, standardized thrice vs potassium acid phthalate (phenolphthalein indicator) just before the titration. The pH electrode was standardized just before titration with pH 4.00 and 7.00 standard buffers (Meterpak pHydrion buffers, Microessential Laboratory, NY). Four hours after the titration, the electrode read 4.01 and 7.05, respectively, for the corresponding standard buffers, thus showing no unusual drift or instability of the glass membrane due to MPEG. (However, after 2 months frequent use the electrode behavior was slightly less stable, possibly due to cumulative effects of contact with polymeric material.) Experimental data were plotted as pH measured vs volume (mL) of standardized NaOH titrant delivered (see Figure 2). Readings were taken following each addition after equilibration by stirring for at least 2 min.

For acidimetric titration, **1** was titrated past the equivalence point, and the resulting solution (pH ≈ 10.5) was back-titrated with 2.83×10^{-2} M aqueous HCl (standardized vs NaOH solution) to equivalence and plotted (see Figure 2).

Titrations of **2**-**6** were run similarly. Thus, four samples of **2** (312−407 mg, $(6-8) \times 10^{-3}$ M) in distilled, deionized water (initial pH 3.3−3.4) were titrated in two separate dual runs using two independently standardized aqueous solutions of NaOH ($(5.7-6.2) \times 10^{-3}$ M), and the data were plotted as pH vs milliliters of NaOH (see Figure 3). Similarly, multiple samples (404−546 mg) of **3**−**6** were dissolved in 25 mL of distilled deionized water and titrated with freshly standardized $(4.9-6.1) \times 10^{-3}$ M aqueous NaOH (see Figure 3).

Nonaqueous potentiometric titrations of **4** and **5** vs 3-hydroxybenzoic acid standard were run in DMSO solvent as described by Hansen et al. (*8*). Thus, 6.0×10^{-2} M solutions of 3-hydroxybenzoic acid (207.2 mg) in DMSO (25 mL) and 786.5 mg of **4** (or 783.1 mg of **5**) in 25 mL of anhydrous DMSO were titrated with a 0.39−0.40 M solution of KOH in methanol (under N_2), delivered from a 2 mL buret. For "pH" in nonaqueous solutions, the pH electrode potential (mV) was recorded (relative to an arbitrary initial point) to construct the titration curves of Figure 4. The absolute potential (E) at other pH was calculated using the Nernst equation, $\text{pH} = (E - 0.2802)/0.059$, with an electrode potential defined relative to a standard calomel electrode (*33*). Immediately before the nonaqueous titrations, the pH meter was standardized (reproducibly) with aqueous buffers at pH 4.00 (+193.4 mV) and 7.41 (−5.5 mV). In graphs of E (mV) vs milliliters of titrant, we offset the pH meter readings by about −123 to −127 mV to plot values relative to an arbitrary 0 mV.

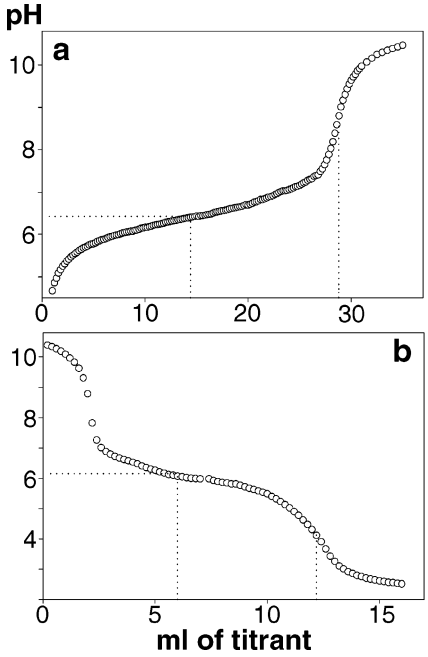

FIGURE 2: Panel a shows potentiometric titration of MPEG-S−bilirubin (**1**) (504 mg/25 mL of water) with standardized 1.06×10^{-2} M aqueous NaOH at 23 °C plotted as pH (vertical axis) vs milliliters of titrant added (horizontal axis). The equivalence point lies near 28.8 mL (dotted line) from which the half-equivalence point (14.4 mL) and average pK_a (6.42) of the two carboxyl groups are determined. Panel b shows acidimetric titration of ionized MPEG-S−bilirubin (**1**) from pH 10.5 with standardized 2.83×10^{-2} M aqueous HCl plotted as pH (vertical axis) vs milliliters of titrant added (horizontal axis). The dotted lines give the equivalence point at 12.2 mL and half-equivalence point at 6.1 mL, corresponding to an average pK_a of 6.15. Sigma Plot analyses (courtesy of Prof. William Kurtin, Trinity University) and visual inspection gave the same values.

Beer's Law Plots. Absorbance (max) values from UV−visible spectra (for example, Figure 5), measured at 23 °C over a wide concentration range in $CHCl_3$ and DMSO solvents, were plotted vs concentration for the intense ∼450 nm long wavelength absorption (Figure 6) as described previously (*34*): (1) A UV−visible spectrum was measured at an appropriate sample concentration in a 10-mm path length cuvette to give an absorbance (A_{max}) of 0.5−0.7, and the molar extinction coefficient (ϵ_{max}) at the maximum absorbance (A_{max}) was calculated. (2) From the ϵ_{max} value thus obtained, the concentration required to give an absorbance of 2 for a path length of 0.5 mm was calculated, and a solution at this concentration was prepared, and its spectrum was measured. A series of dilutions (down to the lowest detection limit of the instrument) was then made from this concentrate, and spectra were measured using cells of appropriate path length from 0.5 to 10 mm. (3) A_{max} data from these spectra were normalized to a path length of 1 cm and plotted vs concentration. (4) To obtain the straight line according to Beer's Law, the adjusted A_{max} values (see step 3) were plotted vs concentration, assuming a constant ϵ_{max}.

Ultracentrifugation Sedimentation Equilibrium. Solutions of bilirubin in aqueous buffers (Tris or EPPS, both from Sigma) were prepared by dissolving an accurately weighed (microbalance) sample of pigment in 2−3 drops of 0.1 M

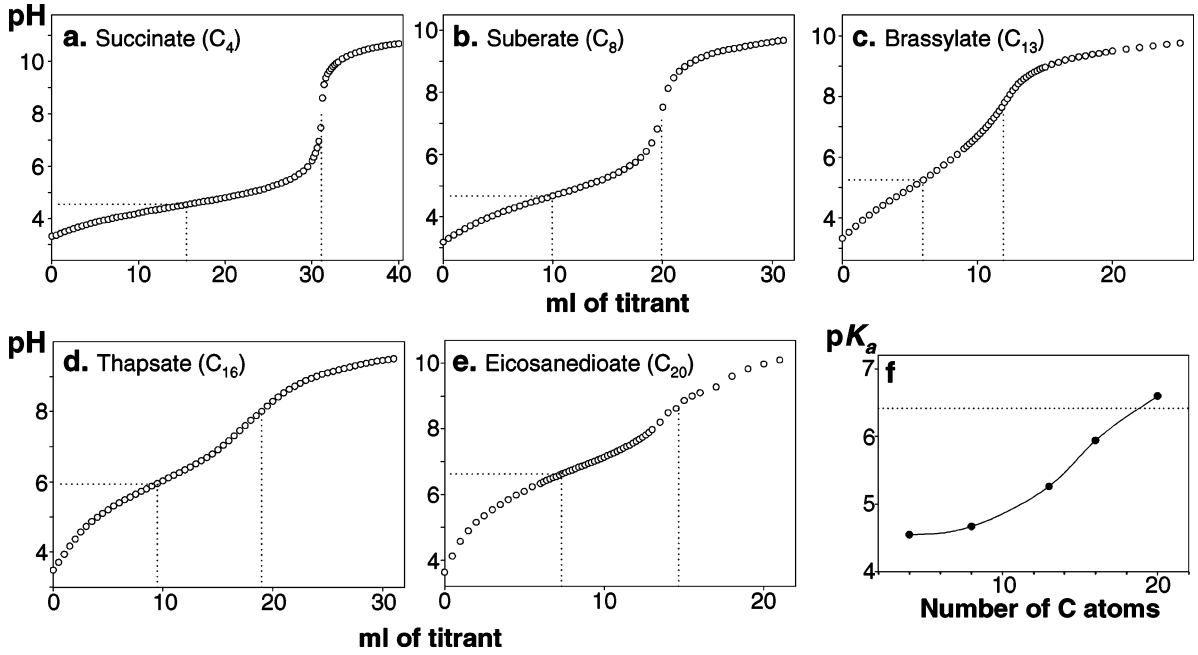

FIGURE 3: Potentiometric titrations (at 23 °C), plotted as pH (vertical axis) vs milliliters of titrant added (horizontal axis) of (a) MPEG-*O*-succinate **2** (407 mg/25 mL of water) with standardized 6.23×10^{-3} M aqueous NaOH (dotted lines give the equivalence point at 31.1 mL and half-equivalence point at 15.6 mL, corresponding to a pK_a of 4.56), (b) MPEG-*O*-suberate **3** (533 mg/25 mL of water) with standardized 5.78×10^{-3} M aqueous NaOH (dotted lines give the equivalence point at 19.9 mL and half-equivalence point at 9.95 mL, corresponding to a pK_a of 4.67), (c) MPEG-*O*-brassylate **4** (429 mg/25 mL of water) with standardized 5.25×10^{-3} M aqueous NaOH (dotted lines give the equivalence point at 11.9 mL and half-equivalence point at 5.95 mL, corresponding to a pK_a of 5.26), (d) MPEG-*O*-thapsate **5** (460 mg/25 mL of water) with standardized 6.10×10^{-3} M aqueous NaOH (dotted lines give the equivalence point at 19.0 mL and half-equivalence point at 9.5 mL, corresponding to a pK_a of 5.94), (e) MPEG-*O*-eicosanedioate **6** (404 mg/25 mL of water) with standardized 5.25×10^{-3} M aqueous NaOH (dotted lines give the equivalence point at 14.6 mL and half-equivalence point at 7.3 mL, corresponding to a pK_a of 6.60). Panel f shows a plot relating the increase in pK_a with lengthening acid chain of fatty acids **2**−**6**. The dotted line at pK_a = 6.42 represents the pK_a of bilirubin−MPEG conjugate **1** obtained from potentiometric aqueous titration.

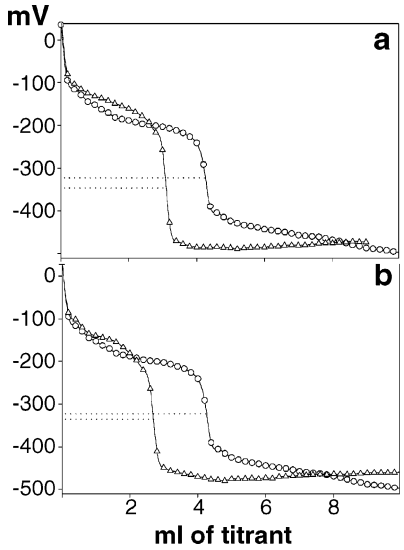

FIGURE 4: Panel a shows the potentiometric titration of **4** (△, 787 mg/25 mL of anhydrous DMSO) and 3-hydroxybenzoic acid (○, 207 mg/25 mL of anhydrous DMSO) with 0.4 M KOH in CH_3OH at 23 °C. The dotted lines represent potential at equivalence at −322 and −345 mV for 3-hydroxybenzoic acid and **4**, respectively. Panel b shows the potentiometric titration of **5** (△, 783 mg/25 mL of anhydrous DMSO) and 3-hydroxybenzoic acid (○, 207 mg/25 mL of anhydrous DMSO) with 0.4 M KOH in CH_3OH at 23 °C. The dotted lines represent potential at equivalence at −322 and −335 mV for 3-hydroxybenzoic acid and **5**, respectively.

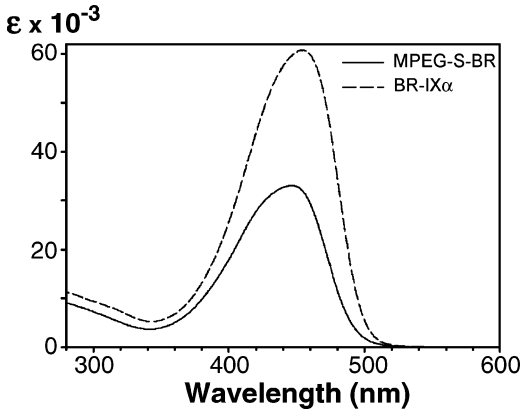

FIGURE 5: UV-visible spectrum of (—) 1.38×10^{-5} M solution of MPEG-S−BR (**1**) and (− − −) 1.72×10^{-5} M bilirubin (BR−IXα) in $CHCl_3$ solvent at 23 °C. The wavelengths at maximum absorption (λ_{max}) for 1.38×10^{-5} M **1** (average molecular weight 2520) are 446 nm (ϵ = 32 900) in $CHCl_3$, 441 nm (ϵ = 32 800) in DMSO, 435 nm (ϵ = 30 000) in pH 8.00 0.5 M aqueous phosphate buffer, and 437 nm (ϵ = 27 800) in water; those for 1.72×10^{-5} M bilirubin IXα are 454 nm (ϵ = 60 400) in $CHCl_3$, 456 nm (ϵ = 63 600) in DMSO, and 440 nm (ϵ = 55 500) in pH 8.00 0.5 M phosphate buffer. The β-mercaptoethanol adduct at the *exo*-vinyl of bilirubin IXα has λ_{max} 449 nm in $CHCl_3$ [Manitto, P., and Monti, D. (1972) *Experientia 28,* 379−380].

NaOH and diluting with argon-saturated Tris (or EPPS) buffer (0.1, 0.2, or 0.05 M) to give 50 mL of the desired solution ($(1.0-6.8) \times 10^{-5}$ M) at various pH. Solutions of bilirubin in $CHCl_3$ or DMSO were prepared by dissolving accurately weighed samples in 10 mL of solvent to give solutions of 1.6×10^{-5} to 4.5×10^{-4} M for $CHCl_3$ and $(1.2-2.0) \times 10^{-5}$ M for DMSO. A model E Beckman analytical centrifuge with an AnD rotor was used for the sedimentation equilibrium measurements: rotor speed 52 000

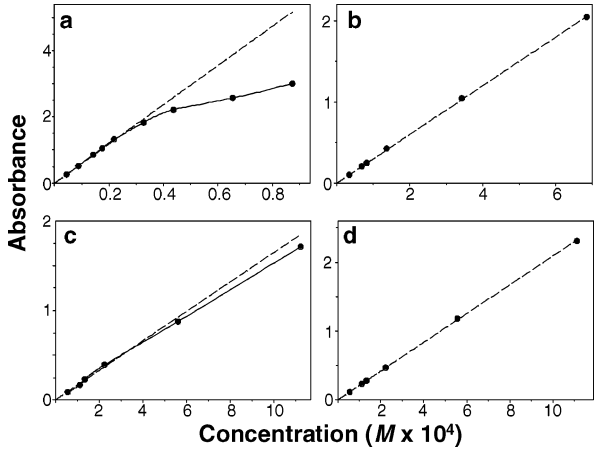

FIGURE 6: Beer's Law plots of absorbance vs concentration for bilirubin in (a) $CHCl_3$ and (b) DMSO and for MPEG-S−BR (**1**) in (c) $CHCl_3$ and (d) DMSO. The dashed lines show the expected Beer's Law plot.

rpm; temperature, 21 °C for aqueous solutions, 19.5−21.5 °C for $CHCl_3$ solutions, 24.5 °C for DMSO solutions. Cells were fitted with sapphire and quartz windows and either KelF or aluminum centerpieces. Aluminum centerpieces with KelF gaskets were used with organic solvents. High speeds in the centrifuge can produce distortions in the optical properties of the windows. Control experiments at the run speeds did not reveal any measurable deviations in absorbance at the wavelengths used for the experiments. The times required to reach equilibrium were typically 12−16 h for aqueous solutions and 5−6 h for $CHCl_3$ and DMSO solutions. UV−visible detection of concentration in the cell was scanned from top to bottom at 500 nm or in some runs at both 500 and 390 nm. Data were not corrected for changes in molar absorptivity accompanying self-association.

A particle placed in an artificial gravitational field generated by ultracentrifugation (*35*) will move from one section of the ultracentrifuge cell to another by the Lamm differential equation (*36*), which is dependent only on sedimentation and diffusion (*35*, *37*):

$$\frac{\partial c}{\partial t} = \frac{\partial}{r\,\partial r}\left(rD\frac{\partial}{\partial r} - s\omega^2 c\right) \tag{1}$$

where D is the diffusion coefficient, r is distance measured from the axis of rotation, ω is angular velocity, c is concentration, and s is the sedimentation coefficient. After a given period, equilibrium is established, where $\partial c/\partial t = 0$, thus giving

$$0 = s\omega^2 rc - D\left(\frac{\partial c}{\partial r}\right) \tag{2}$$

Introducing the "Svedberg equation" (eq 3) into eq 2 gives a formula (eq 4) that can be used to calculate molecular weights (M) in solution.

$$M = \frac{sRT}{D(1-\bar{v}\rho)} \tag{3}$$

$$M = \frac{\partial c/\partial r}{rc}\frac{RT}{\omega^2(1-\bar{v}\rho)} \tag{4}$$

Here, ρ is the density, and $\bar{v}$ is the partial specific volume

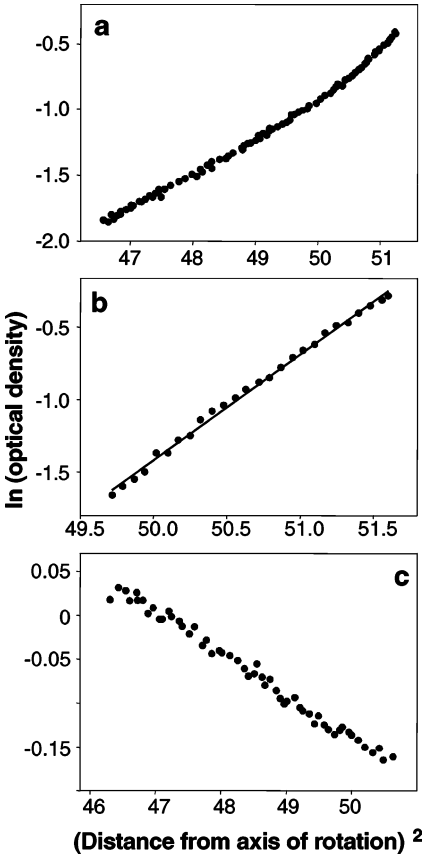

FIGURE 7: Representative plots of ln(OD) (vertical axis) vs r^2 of data taken from the ultracentrifugation sedimentation equilibrium studies of bilirubin: (a) pH 8.5 Tris buffer with data plotted along the length of the scanning window (entry 3 of Table 6); (b) pH 8.5 Tris buffer showing data from another experiment (entry 1 of Table 6) plotted over the constant slope region from which a least-squares fit gave the aggregation number; (c) $CHCl_3$ (see entry 3 of Table 7). Note that the slope of the plot is negative in panel c and positive in panels a and b, which indicates that the solute in panel c is less dense than the $CHCl_3$ solvent ($\bar{v}\rho > 1$).

of the solution. Integrating eq 4 over the length of the ultracentrifuge cell yields the expression 5,

$$\bar{M} = \frac{2RT}{\omega^2(1-\bar{v}\rho)}\frac{\Delta \ln(c)}{\Delta r^2} \tag{5}$$

where $\bar{M}$ is the weight-average molecular weight. The partial specific volume is defined (*38*, *39*) as

$$\bar{v} = \left(\frac{\partial V}{\partial g}\right)_{g\to 0} \tag{6}$$

and can be calculated (*39*) from eq 7.

$$\bar{v} = \frac{1}{\rho} - \left(\frac{1-w}{\rho m}\right)\frac{\mathrm{d}m}{\mathrm{d}w} \tag{7}$$

where w is the weight fraction of solute and m is the weight of solvent and solute.

A plot of ln(c) or ln(OD) vs r^2 (Figure 7) will give a slope that when put into eq 5 gives only a reduced molecular weight when the buoyancy term, $1-\bar{v}\rho$, is not known. Given the partial specific volume, $\bar{v}$, one can then obtain the weight-average molecular weights, $\bar{M}$.

To determine $\bar{v}$, we used a Paar microdensitometer. The density, ρ, of bilirubin in the solvents of interest was

measured on the microdensitometer, and the apparent volume (ϕ) was calculated (*40*) at several bilirubin concentrations for each solvent from the equation

$$\phi = \frac{1}{\rho^0} - \left[\frac{1000\left(\frac{\rho^1}{\rho^0} - 1\right)}{cM}\right] \quad (8)$$

where ρ^0 is density of pure solvent, ρ^1 is density of solvent plus solute, c is concentration, and M is molecular weight of bilirubin. The apparent volume when extrapolated to zero concentration gives the partial specific volume. For Tris buffer, $\bar{v} = 0.720$; for Tris−60% ethanol, $\bar{v} = 0.669$; for Tris−80% ethanol, $\bar{v} = 0.651$; for $CHCl_3$, $\bar{v} = 0.755$; for DMSO, $\bar{v} = 0.760$. Using eq 5 and the reduced molecular weight of bilirubin in $CHCl_3$ (63.5), one calculates $\bar{v} = 0.747$ for monomeric bilirubin in solution, a value in good agreement with the experimentally derived number from microdensitometry. [The reduced molecular weight of bilirubin varies with solvent density (ρ) and is given by the product of the buoyancy term ($1 - \bar{v}\rho$) and the formula weight (584.7) of the pigment.] The corrected weight-average molecular weights were then calculated. The error associated with $\bar{v}_{exp}$ and the reduced molecular weights is approximately 3%.

RESULTS

Compounds **1**−**6** are insoluble in diethyl ether but freely soluble in H_2O, $CHCl_3$, CH_2Cl_2, CH_3OH, and DMSO, giving transparent solutions with no apparent Tyndall effect. The solubility properties of the MPEG-SH conjugate of bilirubin (**1**) differ considerably from those of unconjugated bilirubin, which is very insoluble in H_2O and CH_3OH. The MPEG monoester conjugates (**2**−**5**) are also much more soluble in H_2O than their dicarboxylic acid precursors, which, except for succinic acid, are insoluble in H_2O. When a lower molecular weight poly(ethylene glycol) monomethyl ether, for example, average MW 750, was used for synthesis, the thiol conjugate with bilirubin was insoluble in water. A mechanical mixture of bilirubin and MPEG-SH on contact with water left orange flakes of bilirubin and a colorless filtrate of MPEG-SH, indicating that a covalent bond between polymer and pigment is required for water solubility.

Compounds **1**−**6** gave satisfactory ^{13}C NMR and ^1H NMR spectra, revealing all carbons and protons of both the MPEG and attached acid components (Tables 1 and 2). Evidence for the expected Markovnikov addition (*31*) of MPEG-SH to the *exo*-vinyl group of bilirubin was found in the presence of one upfield doublet for the newly formed methyl of the C(18)−CH(CH_3)S−MPEG moiety of **1**. There was no indication of the bis-adduct of bilirubin-IIIα originating from acid-catalyzed constitutional isomerization (scrambling) (*41*) or bilirubin-IIIα in the starting material. The olefinic region was also very clean, showing three well-resolved proton signals for the remaining *endo*-vinyl group, and two signals for C(15)−CH═ and for C(5)−CH═. The carbon spectrum in $CDCl_3$ exhibited signals in accord with the structure, in particular, the absence of the two olefinic signals and appearance of two new aliphatic carbon signals. Similarly, the DMSO-d_6 NMR spectra were also consistent with a polymer-bound bilirubin. In all ^1H or ^{13}C NMR spectra in $CDCl_3$ and DMSO-d_6, the signal-to-noise ratio was excellent for solutions containing 38 mg mL^{-1} (~1.5×10^{-2} M assuming only one species present).

Table 1: ^{13}C NMR Chemical Shifts and Assignments for MPEG-S−BR (**1**) and Bilirubin

	MPEG-S−BR (**1**)		bilirubin	
carbon	$(CD_3)_2SO$	$CDCl_3$	$(CD_3)_2SO$[a]	$CDCl_3$
1-CO	171.28	174.07	171.34	174.18
19-CO	170.13	173.07	170.41	173.49
2-	123.36	124.51	123.24	124.45
18-	123.20	124.26	122.39	124.38
2-CH_3	9.65	10.09	9.49	10.16
18-CH═CH_2			127.10	125.87
18-CH═CH_2			117.11	118.45
3-	140.35	141.44	140.40	141.57
17-	141.93	142.70	141.97	141.61
3-CH═CH_2	127.36	126.66	127.38	126.77
3-CH═CH_2	122.02	122.29	122.09	122.31
17-CH_3	9.47	10.09	9.26	10.13
4-	127.43	127.71	127.47	127.86
16-	127.96	128.03	128.22	128.88
5-CH═	99.06	101.75	99.15	102.03
15-CH═	99.11	102.04	100.04	102.11
6-	122.02	123.48	122.07	123.55
14-	122.04	124.11	122.25	123.64
7-	119.50	119.55	119.58	119.66
13-	119.50	119.58	119.80	119.80
7-CH_3	9.10	9.17	9.14	9.20
13-CH_3	9.12	9.93	9.16	9.65
8-	123.39	124.54	123.46	124.57
12-	123.39	124.59	124.13	124.75
8^1-CH_2	19.44	18.47	19.25	18.56
12^1-CH_2	19.44	18.47	19.25	18.56
8^2-CH_2	34.26	32.50	34.19[b]	32.59
12^2-CH_2	34.26	32.50	34.24[b]	32.59
8^3-*C*OOH	173.90[b]	179.54	173.95[b]	179.62[b]
12^3-*C*OOH	173.93[b]	179.54	173.96[b]	179.64[b]
9-	130.78	133.47	130.73	133.51
11-	128.36	133.71	131.48	133.95
10-CH_2	23.57	22.18	23.65	22.29
18-CH(CH_3) SMPEG	37.86	38.23		
18-CH(*C*H_3) SMPEG	19.22	19.32		
18-CH(CH_3)-S*C*H_2-	33.85	33.83		
$(CH_2CH_2O)_n$	69.75	70.47		
CH_3-O*C*H_2*C*H_2-O-	58.01	58.98		

[a] Assignments are according to Müller, N. (1985) *Magn. Res. Chem. 23*, 688−689. [b] Interchangeable.

Comparisons of the chemical shifts of key pyrrole and lactam N*H*s and COO*H* ^1H NMR signals, as well as the amide and acid carbonyl ^{13}C atoms of MPEG-S−BR (**1**) with those reported in the literature for bilirubin (*42*) are shown in Table 3. The striking similarity of *all* observed chemical shifts to those of unconjugated bilirubin is a good indication that in $CDCl_3$ and DMSO-d_6 solvents the conformations of the polymer-bound tetrapyrrole and the free pigment are the same. Thus the random coil polymer chain probably does not interfere appreciably with the intramolecular conformation-determining forces in the pigment. Further, it appears that the polymer chain is not involved in steric repulsions with crucial points of conformational flexibility such as the C(10)−CH_2 and C(8), C(12)−CH_2CH_2− fragments. Most importantly, the presence of the pendant polymer does not disrupt the stabilizing network of six intramolecular hydrogen bonds.

Surprisingly, NMR spectra of a 38 mg mL^{-1} aqueous (distilled H_2O, pH ~7) solution of **1** (somewhat more viscous than in DMSO-d_6 or $CDCl_3$, but still completely transparent) did not show any of the ^1H or ^{13}C signals of the pigment.

Table 2: ^{1}H NMR Chemical Shifts, Multiplicities, and Assignments for MPEG-S−BR (**1**) and Bilirubin

	MPEG-S−BR (**1**)		bilirubin	
proton	$(CD_3)_2SO$	$CDCl_3$	$(CD_3)_2SO$	$CDCl_3$[a,b]
8^3,12^3-COOH	11.89	13.61	11.89	13.69
21-NHCO	10.02	10.80	10.02	10.80
24-NHCO	9.84	10.71	9.90	10.69
22-NH	10.39	9.25	10.43	9.27
23-NH	10.43	9.25	10.47	9.30
2-CH_3	1.91	1.98	1.91	1.98
3-CH_X=CH_2	6.80[c]	6.61[j]	6.81[r]	6.61[y]
trans 3-CH=CH_AH_B	δ_A 5.63[d]	δ_A 5.60[k]	δ_A 5.62[s]	δ_A 5.60[z]
cis 3-CH=CH_AH_B	δ_B 5.61[e]	δ_B 5.58[l]	δ_B 5.60[t]	δ_B 5.58[aa]
5-CH=	6.08	6.20	6.08	6.21
15-CH=	6.00	6.10	6.08	6.13
7-CH_3	1.99	2.16	1.99	2.16
8^1, 12^1-CH_AH_X	2.41[f]	δ_X 2.58,[m] δ_A 3.02[n]	2.42[u]	δ_X 2.57,[ab] δ_A 3.01[ac]
8^2, 12^2-CH_BH_C	1.95[f]	2.84[o]	1.93[u]	δ_B 2.90,[ad] δ_C 2.79[ae]
10-CH_2	3.97	4.07	3.98	4.07
13-CH_3	2.01	2.15	2.02	2.15
17-CH_3	2.16	2.16	2.15	2.18
18-CH_X=CH_2			6.56[v]	6.49[af]
trans 18-CH=CH_AH_B			δ_A 5.28[w]	δ_A 5.36[ag]
cis 18-CH=CH_AH_B			δ_B 6.19[x]	δ_B 6.16[ah]
18-C*H*$(CH_3)SCH_2$−	4.03[g]	4.02[p]		
18-CH(C*H*$_3$)SCH_2−	1.49[h]	1.54[q]		
18-CH(CH_3)SC*H*$_2$−	2.56[i]			
$(CH_2CH_2O)_n$	3.50	3.64		
cap C*H*$_3$O−	3.23	3.37		

[a] The assignment follows that in Kaplan, D., and Navon, G. (1983) *Isr. J. Chem. 23*, 177−186, and the *J* constants of the methylene protons in propionic acid chains are taken from spin simulation in Navon, G., Frank, S., and Kaplan, D. J. (1984) *J. Chem. Soc., Perkin Trans. II*, 1145−1149. [b] The assignment of protons in 3-*endo* and 18-*exo* vinyl groups follows that in Kaplan, D., and Navon, G. (1981) *J. Chem. Soc., Perkin Trans. II*, 1374−1383. [c] dd, ^3J = 11.8 Hz, 17.6 Hz. [d] $^2J_{AB}$ = 1.7 Hz, $^3J_{AX}$ = 11.8 Hz. [e] $^2J_{AB}$ = 1.7 Hz, $^3J_{BX}$ = 17.6 Hz. [f] t, *J* = 7.6 Hz. [g] q, *J* = 7.1 Hz. [h] d, *J* = 7.1 Hz. [i] t, *J* = 6.4 Hz. [j] dd, ^3J = 12.0 Hz, 17.3 Hz. [k] $^2J_{AB}$ = 1.3 Hz, $^3J_{AX}$ = 12.0 Hz. [l] $^2J_{AB}$ = 1.3 Hz, $^3J_{BX}$ = 17.3 Hz. [m] 2.54−2.62 ppm, m. [n] 2.95−3.06 ppm, m. [o] 2.79−2.90 ppm, m. [p] q, *J* = 6.9 Hz. [q] d, *J* = 6.9 Hz. [r] dd, ^3J = 11.8 Hz, 17.5 Hz. [s] $^2J_{AB}$ = 1.7 Hz, $^3J_{AX}$ = 11.8 Hz. [t] $^2J_{AB}$ = 1.7 Hz, $^3J_{BX}$ = 17.5 Hz. [u] t, *J* = 7.8 Hz. [v] dd, ^3J = 11.6 Hz, 17.5 Hz. [w] dd, $^2J_{AB}$ = 1.8 Hz, ^3J = 11.6 Hz. [x] dd, $^2J_{AB}$ = 1.8 Hz, ^3J = 17.5 Hz. [y] dd, ^3J = 12.0 Hz, 17.5 Hz. [z] $^2J_{AB}$ = 1.8 Hz, $^3J_{AX}$ = 12.0 Hz. [aa] $^2J_{AB}$ = 1.8 Hz, $^3J_{BX}$ = 17.5 Hz. [ab] ABC*X*, $^2J_{AX}$ = −14.9 Hz, $^3J_{BX}$ = 2.6 Hz, $^3J_{CX}$ = 4.7 Hz. [ac] *A*BCX, $^2J_{AX}$ = −14.9 Hz, $^3J_{AB}$ = 12.9 Hz, $^3J_{AC}$ = 2.8 Hz. [ad] *AB*CX, $^2J_{BC}$ = −18.8 Hz, $^3J_{AB}$ = 12.9 Hz, $^3J_{BX}$ = 2.6 Hz. [ae] *ABC*X, $^2J_{BC}$ = −18.8 Hz, $^3J_{AC}$ = 2.8 Hz, $^3J_{CX}$ = 4.7 Hz. [af] dd, ^3J = 11.5 Hz, 17.7 Hz. [ag] dd, ^2J = 2.0 Hz, ^3J = 11.5 Hz. [ah] dd, ^2J = 2.0 Hz, ^3J = 17.7 Hz.

The MPEG polymer signals were, however, within the normal line-width and had the usual relaxation times. Increasing the relaxation delay between ^{13}C-pulses offered no improvement with respect to the pigment component, nor did warming the solution to 80 °C. Addition of $CDCl_3$ to the NMR tube, to effect partial pigment extraction into $CDCl_3$ from H_2O, led to an almost solid emulsion in the upper (aqueous) layer but showed (by ^{1}H NMR) that the pale yellow $CDCl_3$ lower layer contained the same MPEG-bound bilirubin as if it had been dissolved directly into $CDCl_3$. In a separate experiment, the ^{1}H NMR signals of the pigment reappeared sharply when a fresh aqueous (D_2O) sample was made strongly alkaline (pH >12) with NaOD/D_2O. For this sample, the ^{13}C NMR spectrum of the pigment was also acquired without difficulty. However, solutions of **1** in D_2O−$(CD_3)_2SO$, 9:1 and 1:1 by vol, did not yield ^{1}H or ^{13}C NMR signals for the bilirubin moiety of **1**, although signals from the MPEG moiety were fully evident. Likewise, no ^{1}H or ^{13}C NMR signals from the pigment moiety could be detected from 15 mM samples of **1** dissolved in pH 8.60 phosphate buffer (even after sonication for 1 h) or from samples of **1** dissolved in D_2O (1 mL) in the presence of surfactants above their critical micelle concentrations (cmc), for example, 50 mM sodium dodecyl sulfate (SDS, 14.5 mg/mL) or 4.4 mM cetyltrimethylammonium bromide (CTAB, 4.4 mg/mL). [The cmc of SDS is 8.1−8.4 mM (*43*); that of CTAB is 0.9 mM (*43*)].

Table 3: Comparison of Pyrrole, Lactam, and Carboxylic Acid ^{1}H NMR Chemical Shifts and the Lactam and Carboxylic Acid ^{13}C NMR Chemical Shifts of Poly(ethylene glycol)-Bound Bilirubin (**1**) in $CDCl_3$ and DMSO-d_6 with Those of Bilirubin

signal	$CDCl_3$		DMSO-d_6	
^{1}H NMR	**1**	bilirubin	**1**	bilirubin
pyrrole 22-H	9.25	9.27	10.39	10.43
pyrrole 23-H	9.25	9.30	10.43	10.47
lactam 24-H	10.71	10.69	9.84	9.90
lactam 21-H	10.80	10.80	10.02	10.00
COOH	13.61	13.69	11.89	11.89

signal	$CDCl_3$		DMSO-d_6	
^{13}C NMR	**1**	bilirubin	**1**	bilirubin
19-CONH	173.07	173.49	170.13	170.41
1-CONH	174.07	174.18	171.28	171.34
COOH	179.54	179.62	173.90, 173.93	173.95, 173.96

As with **1**, MPEG monoester acids **2**−**6** gave satisfactory ^{13}C NMR spectra in $CDCl_3$ and $(CD_3)_2SO$ that clearly showed all of the carbon signals of both acid and MPEG moieties. Although their ^{1}H NMR spectra are not as rich as those of **1**, they exhibited the same signals as those of the acid and MPEG components. In contrast to the behavior of **1** in water, the natural isotopic abundance ^{13}C NMR signals of all carbons of **2**−**6** and their ^{1}H NMR resonances could be detected. Unlike the sharp resonance lines seen in $CDCl_3$ and $(CD_3)_2SO$, however, the proton signals of **4** and **6** were very broad in D_2O, those of **6** showing the broadest signals. Similarly, the methylene group ^{13}C resonances of **6** were very broad.

Triplicate potentiometric titrations of **1** led to plots of pH vs milliliters of NaOH titrant as represented by Figure 2a. Acidimetric back-titration of **1** from pH ≈ 10.5 is shown in Figure 2b. Similarly, multiple potentiometric titrations of **2**−**6** gave data from which representative titration curves are shown in Figure 3. From such titration curves, the pH at one-half the volume of titrant delivered to the equivalence point (e.g., see Figure 3a) is equal to the pK_a (or for **1**, the average pK_a of the two carboxyl groups). Thus, we determined the pK_a values of **1**−**6** shown in Table 4. The upward trend of pK_a with increasing chain length is plotted in Figure 3f for **2**−**6**.

Hansen et al. (*8*) have shown how to predict aqueous pK_a's from apparent pK_a's determined in DMSO using an internal standard. Similarly, by comparing the titration curves of 3-hydroxybenzoic acid standard to those of fatty acid half-esters **4** and **5** in DMSO using alkaline methanol as titrant, we obtained plots of millivolts (pH meter reading) vs milliliters of titrant as in Figure 4. From these, we obtained potential difference, ΔE, values of 31.5 and 21.0 mV, respectively, in equivalence points, where $\Delta E = E$(3-hydroxybenzoic acid) − E(**4** or **5**) mV. From the Nernst equation, pH

Table 4: pK_a Values of MPEG-S−Bilirubin (**1**) and MPEG−Acids **2**−**6** from Potentiometric Titrations of Aqueous Solutions

compound	pK_a
1 MPEG-S−Bilirubin	6.42[a]
2 MPEG-$O_2C(CH_2)_2CO_2H$	4.56[b]
3 MPEG-$O_2C(CH_2)_6CO_2H$	4.67
4 MPEG-$O_2C(CH_2)_{11}CO_2H$	5.26
5 MPEG-$O_2C(CH_2)_{14}CO_2H$	5.94
6 MPEG-$O_2C(CH_2)_{18}CO_2H$	6.60

[a] Represents the average value for the two carboxylic acid groups. [b] The pK_a reported for succinic acid monomethyl ester is 4.49 [Kolthoff, I. M., and Chantooni, J. M. K. (1976) *J. Am. Chem. Soc. 98*, 5063−5068].

Table 5: Measured pK_a Values of 3-Hydroxybenzoic Acid in DMSO and Water and MPEG-$O_2C(CH_2)_nCO_2H$ (n = 11, **4**, and n = 14, **5**) in DMSO with Extrapolation[a] to Water

entry	compound	pK_a(DMSO)	pK_a(H_2O)
1	3-hydroxybenzoic acid	5.10	4.06[b]
2	MPEG-$O_2C(CH_2)_{11}CO_2H$ (**4**)	5.63	4.59[c]
3	MPEG-$O_2C(CH_2)_{14}CO_2H$ (**5**)	5.46	4.42[c]

[a] From correcting the pK_a(DMSO) of entries 2 and 3 by ΔpK_a = 1.04 from entry 1. [b] As reported in ref *44*. [c] Note that the potentiometrically measured value of pK_a(H_2O) for **4** is 5.26 and that of **5** is 5.94 (Table 4).

= (E − 0.2802)/0.0591, relating pH to the calomel electrode (*33*), it follows that the potential (E) slopes by 59.1 mV/pH unit (or 59.1 mV/pK_a unit). The 31.5 and 21.0 mV values thus translate into ΔpK_a values of 0.53 and 0.36 for **4** and **5**, respectively, relative to the apparent pK_a (5.1) of the standard in DMSO (*8*). Thus, the apparent pK_a's of **4** and **5** are 5.63 and 5.46 in DMSO. Since the actual aqueous pK_{a1} of 3-hydroxybenzoic acid is 4.06 (*44*), the ΔpK_a between the DMSO and aqueous values is 1.04. Applying this correction to the apparent pK_a's of **4** and **5** in DMSO gave their predicted pK_a's for water as 4.59 and 4.42, respectively (Table 5), just about right for water-soluble aliphatic carboxylic acids (*7*).

The UV−visible spectra of **1** and bilirubin in $CHCl_3$ (Figure 5) are essentially identical, except that the experimental ϵ value of **1** (based on an average molecular weight of 2520) is approximately one-half that of bilirubin, from which we calculate a polymer loading factor of 55%. The small hypsochromic shift with respect to bilirubin-IXα is consistent with saturation of an *exo*-vinyl group. Similar coincident behavior was observed in DMSO. However, Beer's Law plots of **1** and bilirubin in $CHCl_3$, but not DMSO, show the nonlinear behavior characteristic of aggregation (Figure 6), while conformity to Beer's Law is maintained in DMSO solvent.

Information on the molecularity of bilirubin in solution was obtained from ultracentrifugation sedimentation equilibrium studies by plotting ln(OD) vs the square of distance from the axis of rotation (r^2). Representative examples are shown in Figure 7. A straight line indicates that the solution is homogeneous (monodisperse) throughout, that is, it does not contain species of different molecular weights, nor does the solute associate in a concentration-dependent manner. Deviation from a straight line (as in Figure 7a) indicates either heterogeneity or an equilibrium between monomer and oligomers. These possibilities are easily resolved. Different states of aggregation may be observed at the top and the bottom of the centrifuge cell with larger aggregates toward the bottom of the cell. For such heterogeneous solutions, plots of ln(OD) vs r^2 give curved lines, from which each segment can be analyzed separately. In our first experiments on bilirubin in organic solvents, solutions were prepared in pure distilled $CHCl_3$ in volumetric flasks, protected from evaporation by Parafilm and glass stoppering or simply by stoppering with a plastic cap. A striking finding was noted: while those solutions gave a varying slope (as in Figure 7a), a constant slope (as in Figure 7c) was found when Parafilm or plastic caps were avoided or when glass stoppers were rigorously cleansed of traces of grease or detergents. We infer that the presence of adventitious lipid contaminants can cause aggregation of bilirubin in $CHCl_3$. Analysis of extensive ultracentrifugation data at various r distances from top to bottom of the cell, as in Figure 7a, provided estimates of the weight-average molecular weights of bilirubin species in different solvents. Measured values are presented in Tables 6 and 7.

Table 6: Weight-Average Molecular Weights and Aggregation Numbers for Bilirubin in Argon-Saturated Aqueous Buffers at 21 °C

entry	buffer (M)	pH	bilirubin concn ($\times 10^5$ M)	weight-avg molec wt (g mol^{-1})[a]	aggregation number
1	Tris (0.1)	8.5	2.0	3252	5.5_6
2	Tris (0.1)[b]	8.5	2.0	2449	4.1_8
3	Tris (0.1)	8.5	4.2	2189−3754	3.7_4−6.4_3
4	Tris (0.1)[c]	8.5	4.2	1527−2733	2.6_1−4.7_0
5	Tris (0.1)[d]	8.5	4.2	1188	2.0_3
6	Tris (0.1)[e]	8.5	4.2	1196−2646	2.0_5−4.5_3
7	EPPS (0.1)	8.6	4.2	2205	3.7_8
8	Tris (0.1)	9.0	1.0	1132	1.9_4
9	Tris (0.05)	9.1	6.3	1390	2.3_7
10	Tris (0.1)	9.3	6.8	1480	2.5_3
11	Tris (0.2)	9.3	6.6	1460	2.5_0
12	Na_2CO_3 (0.1)	10.0	2.3	1193	2.0_4
13	Na_2CO_3 (0.1)	10.0	2.3	1100	1.8_8
14	Na_3BO_3 (0.1)	10.0	2.3	1150−2350	1.9_7−4.0_2

[a] Single values reflect the average molecular weight across the scanning window of the centrifuge cell; the ranges reported reflect the molecular weights (aggregation) as a function of radius across the same window. For the latter, we performed a more detailed analysis. The molecular weight was determined as a function of radial distance and solute concentration (data not shown). [b] Contains 60% ethanol (v/v) admixed to pH 8.5 Tris buffer. Interestingly, increasing the ethanol concentration to 80% only slightly further reduced the self-association of bilirubin. [c] Same solution as entry 3 after being aged for 4 days in the dark. [d] Solution sonicated for 5 min before commencing ultracentrifugation. [e] Same solution as entry 5 after being aged for 4 days in the dark. Scanned at 390 nm as well as 500 nm.

In aqueous buffers at concentrations from 10 to 70 μM and pH values from 8.5 to 10.0 bilirubin formed dimers or higher aggregates, which were dispersed to some degree by ethanol addition (Table 6). In contrast, bilirubin is monomeric in $CHCl_3$ at ~20 μM (Table 7, entries 1−4), but only if the solvent is pure and free from lipid contamination (Table 7, entries 5−7). DMSO solutions were monomeric at 12 μM with a small amount of aggregation detected at 20 μM.

DISCUSSION

Although bilirubin is classified as a linear tetrapyrrole (*45*), the linear shape (Figure 1a), often depicted incorrectly in textbooks (*5*), is one of the least likely three-dimensional structures in solution. Rather, bilirubin adopts a folded

Table 7: Weight-Average Molecular Weights and Aggregation Numbers for Bilirubin in Chloroform and Dimethyl Sulfoxide Solutions Determined by Ultracentrifugation Sedimentation Equilibrium

entry	solvent	bilirubin concn ($\times 10^5$ M)	temp (°C)	weight-avg molec wt (g mol^{-1})	aggregation number
1	$CHCl_3$	1.6	19.5	568	0.97
2[a]	$CHCl_3$	1.6	19.5	584	1.00
3	$CHCl_3$	2.1	19.5	645	1.10
4[b]	$CHCl_3$	2.2	19.5	559	0.96
5[c]	$CHCl_3$	1.1	21.0	5800	9.9
6[c]	$CHCl_3$	1.8	21.0	6000	10.3
7[c]	$CHCl_3$	35.0	21.0	18650	31.9
8[c]	$CHCl_3$	44.7	21.0	6100−24000[d]	10.4−41.0
9	DMSO	1.2	24.5	540	0.92
10	DMSO	2.0	24.5	615−1276[d]	1.05−2.18

[a] Same solution as entry 1 after 4-day incubation (aging) in the dark. [b] Argon-saturated. [c] Pure distilled chloroform contaminated with traces of adventitious lipid material during handling (see Results). [d] Single values reflect the average molecular weight across the scanning window of the centrifuge cell; the ranges reported reflect the molecular weights (aggregation) as a function of radius across the same window. For the latter, we performed a more detailed analysis. The molecular weight was determined as a function of radial distance and solute concentration (data not shown).

structure shaped like the ridge-tile of a house or a half-opened book (Figure 1b) (*46*, *47*). This conformation is stabilized by intramolecular hydrogen bonding and occurs in crystals of bilirubin (*48*, *49*) and its bisisopropylammonium dicarboxylate salt (*50*). The latter, along with NMR data (*16*), invalidates the idea (*51*) that the dianion may lack internal hydrogen bonding. The ridge-tile secondary structure, with carboxylic acid or carboxylate groups sequestered by intramolecular hydrogen bonds to the opposing dipyrrinones has been shown by extensive spectroscopic studies (*16*, *47*, *52*, *53*) to prevail in solutions of both the diacid and dianion in $CHCl_3$, DMSO, and aqueous buffer at physiological pH, and bilirubin also has the ridge-tile conformation in human serum where it is bound to human serum albumin. Although intramolecular hydrogen bonding stabilizes ridge-tile conformers of bilirubin, this should not be construed as implying that bilirubin or its component dipyrrinones are "rigid" as often suggested (*15*, *24*, *51*). Rather, the pigment is present in solution as a racemic mixture of rapidly interconverting enantiomeric ridge-tile conformers (*54*). These interconvert via trajectories (*47*) that, contrary to earlier proposals (*15*), do *not* require simultaneous rupture of all of the hydrogen bonds or formation of a planar conformation. The ability of bilirubin and its anions to form ridge-tile secondary structures with carboxylic acid (carboxylate) groups sequestered by intramolecular hydrogen bonds to the opposing dipyrrinones explains the considerable lipophilicity of the pigment compared to its biogenetic precursor biliverdin and is a dominant factor in its metabolism, antioxidant behavior, and toxicity. Until about 25 years ago, most estimates and determinations (*8*−*10*, *21*, *55*−*58*) of the acidity constants (K_a's) of bilirubin, though hampered by the insolubility of the pigment, gave values from about 5.0×10^{-5} (pK_a 4.3) to 1.3×10^{-6} M (pK_a 5.9) (Table 8), within the range expected for aliphatic carboxylic acids (*7*). Solvent partitioning studies were consistent with values in this range (*59*). However, subsequent determinations (*12*, *13*, *60*), based on solubility and $CHCl_3$ partition methods, showed markedly elevated pK_a values (p$K_{a_1} \approx 6.8-8.1$; p$K_{a_2} \approx 8.4-9.3$) that matched or exceeded those few exceptions reported in earlier years (*14*, *56*, *58*). These determinations (*12*, *13*, *60*) gave inconsistent results and were run only on bilirubin itself and not validated with other pyrrolic carboxylic acids, biliverdin, or standards. The extraordinarily high pK_a values were attributed to effects of intramolecular hydrogen bonding on COOH dissociation, which generally has only weak effects on the dissociation of neutral aliphatic carboxylic acids (*61*). More recent sensitive ^{13}C NMR studies on ^{13}C-labeled mesobilirubin XIIIα, which is likely to have ionization constants very similar to those of bilirubin, produced values (p$K_{a_1} \approx 4.2$, p$K_{a_2} \approx 4.9$) (*11*, *20*) that fall into the lower, more normal range for propionic acid groups, except in the presence of taurodeoxycholate micelles, where incorporation of the mesobilirubin into or onto taurodeoxycholate micelles caused the pK_a values to rise into the 6−7 range (*62*). Values similar to those of mesobilirubin XIIIα were found for mesobiliverdin XIIIα in which the COOH groups may hydrogen-bond to each other but cannot engage in hydrogen bonding to lactam and pyrrole NH groups as in bilirubin. As expected (*11*), intramolecular hydrogen bonding of the COOH groups had little effect on the dissociation constants of mesobilirubin XIIIα and only a weak effect on those of mesobiliverdin XIIIα. In contrast to the solubility and $CHCl_3$ partition measurements (*12*, *13*, *60*), the ^{13}C NMR measurements were substantiated using a large group of hydrogen-bonded and non-hydrogen-bonded mono-, di- and tetrapyrrole ^{13}C-labeled carboxylic acids and standards of different degrees of water solubility, which yielded self-consistent results (*11*, *20*, *22*). Subsequently, it was suggested that the conventional values are wrong because of aggregation and disruptive solvent effects on intramolecular hydrogen bonding (*12*, *13*, *15*, *24*, *63*) during the measurements, and pK_a values of 8.1 and 8.4 are becoming uncritically accepted in the literature (*15*, *24*, *64*, *65*) and used to formulate new concepts of bilirubin metabolism (*15*).

Table 8: Previously Reported Bilirubin Acidity Constants (pK_a)

apparent pK_a	solvent	method	ref
(4.4 and 5.0)[a]	H_2O	emf,[b] solubility	*55*
7.1	H_2O-CH_3OH	spectrophotometry[c]	*56*
≪7	$H_2O-(CH_3)_2CO$	emf[b]	*57*
7.55	H_2O	emf[b]	*58*
4.3 and 5.4	$(CH_3)_2NCHO$	emf,[b] spectrophotometry[c]	*10*
4.50 and 5.90	H_2O	spectrophotometry[c]	*9*
5.1 (4.4)[e]	$(CD_3)_2SO$[d]	^{13}C NMR,[e] emf,[b] spectrophotometry[c]	*8*
6.7 and 7.5	H_2O	spectrophotometry,[c] solubility	*14*
7.2	$H_2O-CHCl_3$	solvent partition[f]	*60*
6.8 and 9.3	H_2O	solubility	*12*
8.12 and 8.44	$H_2O-CHCl_3$	solvent partition[f]	*13*
4.2 and 4.9	$H_2O-(CH_3)_2SO$	^{13}C NMR[g]	*11*
6.3 and 6.7	$H_2O-(CH_3)_2SO$ + TDC[h]	^{13}C NMR[g]	*62*

[a] Suggested values, not measured experimentally. [b] Potentiometric (emf = electromotive force) titration using a pH meter. [c] UV−visible spectrophotometric titration. [d] Cotitration with hydroxybenzoic acid standards. [e] Extrapolated to pK_a = 4.4 in water from dimethyl sulfoxide using the Born equation. [f] Solvent partition between $CHCl_3$ phase and aqueous buffer phase. Previous solvent partition studies using solvents other than $CHCl_3$ were consistent with pK_a values of ~4.4 and 5.0 (ref *59*). [g] Using 90% enriched $^{13}CO_2H$ in mesobilirubin-XIIIα. [h] Solution is 40 mM in sodium taurodeoxycholate (cmc = 2−4 mM).

Our original goal in these studies was to make a water-soluble bilirubin whose pK_a could readily be measured titrimetrically. We set out to obtain aqueous solubility throughout the pH range 4−10 and to avoid anionic and cationic solubilizing groups to eliminate the possibility of resident electrostatic field effects on carboxylic acid deprotonation. We were attracted to poly(ethylene glycol) (PEG) as a water-solubilizing group because it could be attached covalently in a position remote from the carboxylic acid groups of the pigment. Borrowing from earlier work (*27*, *30*), we converted molecular weight ∼1900 poly(ethylene glycol) monomethyl ether (MPEG-OH) into its terminal thiol and regioselectively added (thiol addition) the reagent to bilirubin to produce **1**, which is soluble in water. To compare the behavior of water-soluble **1** to water-solubilized fatty acids, we also converted a series of dicarboxylic acids (C_4 to C_{20}) to their monoesters (**2**−**6**) with MPEG-OH. All of these compounds were stable and soluble enough in water for accurate titrimetric pK_a measurements.

The titrimetrically measured apparent average pK_a (6.42, Table 4) of water-soluble MPEG-S−bilirubin **1** is clearly numerically greater than the pK_a's (4.2−4.9) measured by the ^{13}C NMR method using DMSO cosolvent (*11*) yet similar to the pK_a's (6.3−6.9) of mesobilirubin in TDC micelles (*62*) (Table 8). However, it is notably lower than the high values reported (*12*, *13*, *60*) for supposedly monomeric bilirubin based on partitioning and solubility measurements (Table 8). The absence of ^{1}H and ^{13}C NMR signals in H_2O or D_2O from the pigment part of **1** (but not the MPEG part, whose NMR signals are seen) suggests that the pigment moiety is not tumbling rapidly on the NMR time scale. This contrasts with the NMR in aqueous solution at pH >12 and in $CDCl_3$ or $(CD_3)_2SO$ solutions, where the ^{13}C NMR signals of the pigment are observed. The data are consistent with aggregation of the bilirubin component of **1** in aqueous solution. Such aggregates are probably micelles with a relatively immobile aggregated bilirubin core surrounded by mobile MPEG tails forming the micellar surface. Our NMR data are consistent with those reported recently (*66*) for bilirubin encapsulated in polymeric nanoparticles made from poly(γ-benzyl L-glutamate) (PBLG)/molecular weight 20 000 poly(ethylene oxide) (PEO) hexablock copolymer (called GEG). The GEG nanoparticle has hydrophobic PBLG as the core and hydrophilic PEO as the shell. In D_2O, encapsulated bilirubin showed no pigment or PBLG ^{1}H NMR signals, which are even easier to detect than natural abundance ^{13}C NMR signals; only the signals from the PEO, more or less broadened, were seen. In contrast, in $CDCl_3$, the characteristic pigment resonances, as well as those of PBLG and PEO, were observed. Such data are consonant with a hydrophobic core of bilirubin and PBLG and a hydrophilic outer shell of PEO in aqueous solution. The parallel to our observations of MPEG-S−bilirubin **1** in water could not be more evident. Thus, the elevated average pK_a of **1** (Table 4) is most probably associated with aggregated rather than monomeric bilirubin, as is the elevated pK_a (∼6−7) of mesobilirubin in taurodeoxycholate micelles (*62*) in which positioning of the carboxyl groups near the micelle surface may allow the surface potential to influence acid dissociation.

We conclude that aggregation *increases* the apparent pK_a's of the carboxyl groups of bilirubin relative to the monomer in water, rather than lowering them, as implied in recent papers (*24*, *63*). This phenomenon is well-known. For example, aggregated alkanoic carboxylic acids are also known to exhibit elevated pK_a values (decreased acidity) relative to the monomers (*17*, *67*−*71*). In a detailed, comprehensive ^{13}C NMR study of fatty acid apparent pK_a's (Table 9), Cistola, Small, and Hamilton and co-workers (*17*, *67*−*69*, *72*) obtained strong evidence that aggregation leads to elevated pK_a values. Thus, while aqueous solutions of low molecular weight aliphatic carboxylic acids gave normal, ordinary pK_a's, as did octanoic acid (near the limit of aqueous solubility), the pK_a of octanoic acid vesicles jumped 1.7 pK units to 6.5, a value nearly reproduced by decanoic acid liquid crystals and soaps. Even more elevated pK_a's (to pK_a ≈ 10.0) were found with stearic acid monolayers (*68*, *70*), whereas stearic acid in phosphatidylcholine single-walled vesicles showed pK_a = 7.2−7.4 (*73*) and comparably high values, pK_a = 7.5−7.9, were found with oleic acid vesicles (*68*). Similar trends were reported recently for porphyrin acids in liposomes (*74*). While we do not believe that fatty acids are appropriate structural analogues for bilirubin, it is clear that aggregation has a qualitatively similar effect on the pK_a's of bilirubin. The generic titration curve for a fatty acid in water sketched by Kanicky and Shah (*70*) is strikingly similar to the automatic titration curve for bilirubin in water published by Krasner and Yaffe (*58*), which yielded an apparent pK_a for bilirubin of 7.55. In that study solutions were bubbled with nitrogen during titrations, which would accelerate aggregation, and precipitation of bilirubin occurred during the titration as it does with long-chain fatty acids. The high apparent pK_a clearly stems from aggregation rather than effects of intramolecular hydrogen bonding on dissociation. We suspect that this pK_a increase on aggregation or "condensation" of bilirubin (for example, in membranes) is of central importance for understanding the uptake of the pigment by cells and the mechanism of kernicterus.

To further calibrate our pK_a data from **1**, we prepared MPEG derivatives of a series of acids from C_4−C_{20} and

Table 9: Low Molecular Weight Carboxylic and Fatty Acid pK_a Values Showing the Effect of Aggregation on Elevating pK_a

	pK_a(H_2O)			
R-$^{13}CO_2H$, R =	apparent (from NMR)	potentiometric	lit. value	lit. ref
CH_3−	4.7	4.6	4.75	*18*, *68*
CH_3CH_2−	4.9	4.8	4.87	*18*, *68*
$CH_3CH_2CH_2$−	4.8	4.8	4.82	*18*, *68*

R-$^{13}CO_2H$, R =	apparent pK_a(H_2O) (from NMR)	form	ref
$CH_3(CH_2)_6$−	4.8	monomers	*68*, *69*
$CH_3(CH_2)_6$−	6.5	vesicles	*68*, *72*
$CH_3(CH_2)_8$−	6.8	liq cryst, >cmc	*68*, *72*
$CH_3(CH_2)_8$−	6.7	cryst oleic acid soap; 0.08 M in H_2O	*68*, *72*
$CH_3(CH_2)_7$−CH=CH−$(CH_2)_7$−	7.0	cryst oleic acid soap; 0.08 M in H_2O	*68*, *72*
$CH_3(CH_2)_7$−CH=CH−$(CH_2)_7$−	7.9	lamellar, 0.08 M in H_2O	*68*, *72*
$CH_3(CH_2)_7$−CH=CH−$(CH_2)_7$−	7.5	vesicles, 5 mol %	*68*, *72*
$CH_3(CH_2)_7$−CH=CH−$(CH_2)_7$−	7.6	vesicles, 21 mol %	*68*, *72*
stearic $CH_3(CH_2)_{16}$−	8.9	monolayers	*68*

determined their pK_a's by potentiometric titration in water (Table 4). As in the ^{13}C NMR study of low molecular weight alkanoic acids (Table 9), the measured pK_a's of **2** and **3** were normal (4.56 and 4.67). However, at the fatty acid level, the pK_a values rose from 5.26 to 6.60 (**4** to **6** of Table 4); see Figure 3f for a plot of pK_a vs chain length. Again, the data are consistent with a fatty acid core aggregate encapsulated by an MPEG vesicle-like nanostructure.

To determine what the pK_a of fatty acids **4** and **5** might have been if their solutions were monomeric, we used a method developed previously (*8*) to determine the mean pK_a of monomeric bilirubin in water. In this method, the pigment is titrated together with a reference standard (3-hydroxybenzoic acid) in DMSO solution with alkaline methanol, and values for pure water are obtained by extrapolation. The data (Table 5) so obtained suggest a normal pK_a value (4.4−4.6) for monomeric **4** and **5** in water, which contrasts with the higher observed pK_a's (5.26 and 5.94) determined by direct potentiometric titration in water. We take this as evidence for aggregation of aqueous **4** and **5**, and by extension other fatty acids, and also as validation for the pK_a of bilirubin previously reported (*8*). The clearly emerging picture is that the pK_a's of aggregatable carboxylic acids, including bilirubin, are highly dependent on the state of aggregation of the acid. Whereas monomeric bilirubin has a normal mean pK_a (∼5 pK units), aggregated bilirubin exhibits elevated pK_a's (>5).

These studies on pegylated fatty acids, along with earlier ^{13}C NMR investigations, provide further compelling evidence for the reliability of the ^{13}C NMR method used previously to estimate the acid dissociation constants of bilirubin and biliverdin.

Evidence for aggregation of bilirubin/bilirubinate in aqueous solution (*21*, *75*−*79*) has been discussed in detail by Carey and Spivak (*79*). Our studies, summarized in Table 6, show that the pigment is aggregated in pH ≤ 8.5 buffers and that the lower the pH, the more highly it is aggregated. Entry 1 in Table 6 (from Figure 7b) indicates a weight-average molecular weight in pH 8.5 buffer that corresponds to a hexamer that is only partly dissociated upon admixture with ethanol (entry 2). Subsequent independent evaluations (entry 3 from Figure 7a) gave an average aggregation range of 3.7−6.4 (distributed from top to bottom of the centrifuge cell). When the solution was aged, the values shifted to 2.6−4.7, consistent with the fact that our initial hexamer (entry 1) predominated in freshly prepared solutions with ultracentrifugation started immediately. Even over time, however (entry 4), bilirubinate solutions in pH 8.5 aqueous buffer are not monomeric. Entry 5 shows that after ultrasonication (to disperse aggregates), the pigment is still dimeric at pH 8.5 and that aging (entry 6) leads to reassociation to nearly the aggregation levels seen in entry 4. A change of pH 8.5 buffer from Tris to EPPS (entry 7) had little effect on aggregation. At higher pH (≥9.0), however, as predicted by Brodersen (*21*, *75*, *76*) and Carey (*78*, *79*) and co-workers, buffered bilirubin solutions tend toward dimeric (entries 8−11), irrespective of pigment or buffer concentration. At the highest pH studied (10.0), the ionized bilirubin was dimeric (entries 12−14), although there is evidence here, too, for a range of aggregates (entry 14), the main aggregation state being dimeric. One might reasonably expect that metastable solutions of bilirubin in pH 7.2−8.0 aqueous buffers will be highly aggregated but that added organic cosolvents such as ethanol or DMSO might decrease the state of aggregation as observed in other systems (*80*). In vivo, endogenous solutes in tissue fluids may inhibit aggregation or facilitate disaggregation of the pigment.

We also studied the state of aggregation of bilirubin in $CHCl_3$ and DMSO, two common bilirubin solvents. Entries 1−4 of Table 7 confirm that bilirubin is monomeric in $CHCl_3$ at $(1-2) \times 10^{-5}$ M, but entries 5−8 caution that serious aggregation can be induced in $CHCl_3$ by the presence of trace quantities of impurities that might be leached adventitiously from cap liners, stopcocks, stoppers, grease, Parafilm, or containers previously washed with detergent. In DMSO (entries 9, 10), the data show a mainly monomeric solution with possibly a small fraction of dimers. Bilirubin dimers appear to be moderately stable species, as discussed by Carey and Spivak (*79*).

Thus, bilirubin is mainly aggregated in water and in alkaline buffers even at pH 10 and (caution!) can become seriously aggregated in $CHCl_3$. It confirms that aggregates of bilirubin tend to exhibit exalted pK_a values, as do aggregates of fatty acids, relative to monomeric species. The observation that bilirubin aggregates predominate in aqueous solution and occur relatively easily in $CHCl_3$ suggests caution and circumspection when using such systems, especially for pK_a determinations.

^{13}C NMR-based estimates of the pK_a's of bilirubin in water have been dismissed as inaccurate (too low) because of supposed aggregation (*24*, *63*). The present studies do not support that view and show that aggregation would, if anything, *increase* pK_a rather than lower it as observed with other carboxylic acids. Our observations suggest that the anomalously high reported (*12*, *13*) pK_a values themselves may be artifacts of aggregation. Such aggregation phenomena have also been detected and analyzed independently using a principal compound analysis from pH-dependent UV−visible spectra (*81*) and have long been recognized as potential sources of error and spuriously high values in measurements of the pK_a's of bilirubin. An advantage of solution-NMR experiments (*67*) is that ^{13}C NMR signals are detected only from dissolved pigment. Monomers, or dissolved multimers when present, give chemical shifts that are the population-weighted average of equilibrated entities in the fast exchange NMR regime, but undissolved or colloidal sample is resonance-silent (*66*). Furthermore, aggregation has been shown in alkanoic acid anions to exert only a minor influence on $^{13}CO_2^-$ chemical shifts (*82*), contrary to suggestions (*23*).

Earlier pK_a determinations have also been dismissed as erroneous because they used DMSO or DMF to solubilize the pigments. This dismissal is based on the following two hypotheses (*12*, *13*, *15*, *24*, *51*, *83*−*85*): (1) that intramolecular hydrogen bonding in bilirubin retards dissociation of protons from the carboxyl groups, resulting in high pK_a's and dissociation constants several orders of magnitude different from the usual values; (2) that solvents such as DMSO or DMF break the internal hydrogen bonding, thereby facilitating dissociation and leading to low pK_a's. Both of these notions seem to stem from the incorrect belief (*15*, *24*, *51*) that the hydrogen bonds in bilirubin are fixed and that the molecule has a rigid structure in solution. They overlook the dynamics of the molecule and the fact that it exists in solution as a mixture of rapidly interconverting

enantiomers (*54*) in which the network of weak intramolecular hydrogen bonds is constantly being broken and reformed, allowing for easy dissociation of acidic protons. To what extent are these hypotheses valid?

1. Hydrogen Bonding and Dissociation. The assertion that intramolecular hydrogen bonding retards dissociation of the carboxyl groups may sound plausible, but there is abundant evidence that intramolecular hydrogen bonding per se does *not* have large effects on carboxyl dissociation or lead to markedly elevated pK_a's for neutral species (*61*, *86*). Examples are ethyl maleate, where intramolecular hydrogen bonding actually *lowers* the pK_a relative to ethyl fumarate (*87*), and simple benzoic acids in which intramolecular hydrogen bonding *lowers* pK_a's and micellization increases them (*86*). Other examples where intramolecular hydrogen bonding lowers the first pK_a of a dicarboxylic acid are given in refs *11* and *88*. When intramolecular hydrogen bonding does increase the pK_a of a neutral carboxylic acid (*89*−*91*), increases are generally not more than ∼1.5 pK_a units, much less than the 3−4 units suggested for bilirubin (*13*). This is not to say that pK_a's of ∼8 for simple dicarboxylic acids are not to be found. One example is the dicarboxylic acid *cis*-caronic acid (3,3-dimethyl-*cis*-1,2-cyclopropane dicarboxylic acid), for which pK_{a_2} is 8.1 (*92*). However, such examples invariably involve the dissociation of a carboxyl intramolecularly hydrogen-bonded to a negatively charged entity such as a carboxylate group and are irrelevant to bilirubin in which hydrogen bonding of the two propionic acid groups to each other is energetically unfavorable (*47*). Therefore, the argument that intramolecular hydrogen bonding in bilirubin retards dissociation sufficiently to increase the COOH pK_a's from the normal range of 4−5 to >8 (*13*, *15*) is both implausible and unprecedented. Since the mono- and dianions of bilirubin are themselves stabilized by intramolecular hydrogen bonding (*50*), it would be more likely that the pK_a's of the acid forms would be *lowered* by hydrogen bonding, as in the case of the first pK_a of malonic acid or maleic acid (*92*).

2. Influence of DMF and DMSO on Hydrogen Bonding and pK_a Determinations. Bonnett et al. (*46*) first raised the theoretical possibility that the conformation and hydrogen bonding of bilirubin might be different in polar solvents, such as DMF, than in less polar solvents such as chloroform. But the idea that DMF and DMSO facilitate COOH ionization by breaking internal hydrogen bonding and drastically lower the pK_a of bilirubin seems to have originated with Ostrow and Cohen (*84*) and has been asserted frequently since then (*12*−*14*, *51*). There is, however, scant scientific evidence to substantiate such assertions. The structure of bilirubin in DMF is, in fact, not known, though absorption spectra (*93*) suggest that it is similar to the structure in chloroform. Similarly, absorption spectra indicate that the same ridge-tile structure is present in 100% DMSO. Early NMR and infrared investigations were equivocal on the effect of DMSO on hydrogen bonding, but later relaxation time (T_1) NMR studies in 100% d_6-DMSO led Kaplan and Navon (*53*) to suggest that the bilirubin propionic acids are linked to the dipyrrinones by bound solvent (DMSO) molecules. More recent detailed investigations using improved NMR instrumentation and sophisticated heteronuclear Overhauser effect techniques, along with circular dichroism studies on synthetic optically active bilirubins (*16*, *52*, *94*−*97*), support this view and show clearly that even in 100% DMSO-d_6 an intramolecularly hydrogen-bonded ridge-tile conformation is present. Thus, the current picture is that dissolving bilirubin, mesobilirubin XIIIα, or the tetra-*n*-butylammonium salt of mesobilirubin XIIIα in 100% DMSO does *not* completely break the matrix of intramolecular hydrogen bonds. Of course, in aqueous DMSO solutions such weak effects of DMSO are likely to be greatly attenuated. That is why, in previous pK_a determinations using DMSO as cosolvent (*11*, *20*), we ensured that water was always present in large molar excess. In addition, we ran controls with hydrogen-bonded standards of known pK_a to check that the presence of DMSO did not lead to aberrant values by disrupting hydrogen bonding (*11*, *22*). It is noteworthy that three groups of investigators using three different NMR techniques and solvent systems of widely different hydrogen-bonding properties (DMSO, DMF, and H_2O/DMSO) independently obtained very similar estimates for the pK_a's of bilirubin (*8*, *10*, *11*, *20*). If organic solvent interference with intramolecular hydrogen bonding played such a major role as has been frequently suggested, it is hardly likely that similar values would have been obtained with all three systems.

Thus, the arguments used to question the NMR-based estimates of the acidity constants of bilirubin and to rationalize the high pK_a values obtained by chloroform partitioning are insubstantial and fallacious. This, then, begs the question of why the latter method gave such high values. Our current observations suggest that aggregation, caused by adventitious impurities, may have played some role. This would be consistent with the problems with emulsion formation that were experienced by the investigators (*13*). Yet, aggregation would not be expected to lead to such large elevations of pK_a. Chloroform partitioning is a valid method for measuring pK_a's, and the experiments appear to have been carried out with care. However, as Irollo et al. (*59*) have pointed out, $CHCl_3$ is a poor solvent for partitioning studies with bilirubin in the physiologic pH range because the distribution coefficient so highly favors the organic phase that accurate measurement of the exceedingly low concentration of pigment in the aqueous phase becomes practically impossible. It is noteworthy that the $CHCl_3$ partitioning measurements involved multiple extractions, back-extractions, and transfers of pigment solutions, which are generally to be avoided when working with a hydrophobic, surface-active, somewhat labile pigment like bilirubin. In addition, bilirubin concentrations were measured by the nonspecific and notoriously unreliable diazo procedure, and calculation of the final data required a number of corrections and assumptions about the molecularity of bilirubin in solution, which, in the light of the current findings, are unlikely to be true. An earlier chloroform partitioning study (*60*) from the same laboratories led to quite different pK_a values for bilirubin than 8.1 and 8.4, and a later estimate (*12*) was subsequently retracted because of methodologic problems (*15*, *85*), just as initial measurements of bilirubin/albumin binding affinities by the same groups (*15*, *85*) were also later reported to be erroneous because of technical flaws (*98*). Therefore, we consider it not beyond the bounds of possibility that deficiencies in methodology, in addition to overlooked aggregation, may have contributed to the aberrant pK_a values reported for bilirubin on the basis of chloroform partitioning experiments (*13*, *60*).

CONCLUSION

For years, the aqueous dissociation constants of monomeric bilirubin have been described as uncertain. While highly accurate values are still unavailable, a substantial body of evidence now indicates that they are within the range ($pK_a = 4-5$) expected for aliphatic propionic acid groups, that they are not greatly influenced by intramolecular hydrogen bonding, as expected for this type of carboxylic acid, and that aggregation of the pigment leads to elevated apparent pK_a's. Indeed, unusually high pK_a values in the absence of any structure rationale should lead to a suspicion of some sort of aggregation phenomenon. Published values of >8.0 are no longer credible, and biological models (*15*) based on them may be misleading and erroneous. Estimates of the water solubility of bilirubin based on the same partitioning studies (*13*, *60*) and frequently cited in recent bilirubin literature (*25*, *99*−*102*) may also be incorrect.

ACKNOWLEDGMENT

We sincerely thank Mr. Lewis Cary (University of Nevada, Reno) for help with the NMR experiments. K.W. was an NSF-REU summer undergraduate research trainee.

REFERENCES

1. Blanckaert, N., and Fevery, J. (1990) in *Hepatology* (Zakim, D., and Boyer, T. D., Eds.) pp 254−302, W. B. Saunders Co., Philadelphia, PA.
2. Chowdhury, J. R., Wolkoff, A. W., Chowdhury, N. R., and Arias, I. M. (2001) in *The Metabolic and Molecular Bases of Inherited Disease* (Scriver, C. R., Beaudet, A. L., Sly, W. S., Valle, D., Childs, B., Kinzler, K., and Vogelstein, B., Eds.) pp 3063−3101, McGraw-Hill, Inc., New York.
3. Greenberg, D. A. (2002) The jaundice of the cell, *Proc. Natl. Acad. Sci. U.S.A. 99*, 15837−15839.
4. Sedlak, T., and Snyder, S. H. (2004) Bilirubin benefits: cellular protection by a biliverdin reductase antioxidant cycle, *Pediatrics 113*, 1776−1772.
5. Ritter, S. K. (2003) Mind your *E*'s and *Z*'s. Due diligence by chemists is needed to prevent propagation of structural and other errors. *Chem. Eng. News 81*, 29.
6. Brodersen, R., and Stern, L. (1987) Aggregation of bilirubin in injectates and incubation media: its significance in experimental studies of CNS toxicity, *Neuropediatrics 18*, 34−36.
7. Serjeant, E. P., and Dempsey, B. (1979) *Ionization Constants of Organic Acids in Aqueous Solution*, Pergamon Press, Ltd., Oxford, U.K., and references therein.
8. Hansen, P. E., Thiessen, H., and Brodersen, R. (1979) Bilirubin acidity. Titrimetric and ^{13}C NMR studies, *Acta Chem. Scand. B 33*, 281−293.
9. Kolosov, I. V., and Shapovalenko, E. P. (1977) Acid−base equilibria in solutions of bilirubin, *Zh. Obshch. Khim. 47*, 2149−2151.
10. Lee, J. J., Daly, L. H., and Cowger, M. L. (1974) Bilirubin ionic equilibria; their effects on spectra and on conformation, *Res. Commun. Chem. Pathol. Pharmacol. 9*, 763−770.
11. Trull, F. R., Boiadjiev, S., Lightner, D., and McDonagh, A. F. (1997) Aqueous dissociation constants of bile pigments and sparingly-soluble carboxylic acids by ^{13}C NMR in aqueous dimethyl sulfoxide: effects of hydrogen bonding, *J. Lipid Res. 38*, 1178−1188.
12. Ostrow, J. D., Celic, L., and Mukerjee, P. (1988) Molecular and micellar associations in the pH-dependent stable and metastable dissolution of unconjugated bilirubin by bile salts, *J. Lipid Res. 29*, 335−348.
13. Hahm, J.-S., Ostrow, J. D., Mukerjee, P., and Celic, L. (1992) Ionization and self-association of unconjugated bilirubin, determined by rapid solvent partition from chloroform, with further studies of bilirubin solubility, *J. Lipid Res. 33*, 1123−1137.
14. Moroi, Y., Matuura, R., and Hisadome, T. (1985) Bilirubin aqueous solution. Absorption spectrum, aqueous solubility, and dissociation constants, *Bull. Chem. Soc. Jpn. 58*, 1426−1431.
15. Ostrow, J. D., Mukerjee, P., and Tiribelli, T. (1994) Structure and binding of unconjugated bilirubin: relevance for physiological and pathophysiological function, *J. Lipid Res. 35*, 1715−1737.
16. Nogales, D., and Lightner, D. A. (1995) On the structure of bilirubin in solution. $^{13}C\{^1H\}$ heteronuclear Overhauser effect NMR analyses in aqueous buffer and organic solvents, *J. Biol. Chem. 270*, 73−77.
17. Cistola, D. P., Small, D. M., and Hamilton, J. A. (1982) Ionization behavior of aqueous short-chain carboxylic acids: a carbon-13 NMR study, *J. Lipid Res. 23*, 795−799.
18. Hagen, R., and Roberts, J. D. (1969) Nuclear magnetic resonance spectroscopy. ^{13}C spectra of aliphatic carboxylic acids and carboxylate anions, *J. Am. Chem. Soc. 91*, 4504−4506.
19. Choi, P. J., Petterson, K. A., and Roberts, J. D. (2002) Ionization equilibria of dicarboxylic acids in dimethyl sulfoxide as studied by NMR, *J. Phys. Org. Chem. 15*, 278−286.
20. Lightner, D. A., Holmes, D. L., and McDonagh, A. F. (1996) On the acid dissociation constants of bilirubin and biliverdin. pK_a values from ^{13}C NMR spectroscopy, *J. Biol. Chem. 271*, 2397−2405.
21. Brodersen, R. (1986) in *Bile Pigments and Jaundice* (Ostrow, J. D., Ed.) pp 157−181, Marcel Dekker, Inc., New York.
22. McDonagh, A. F., Phimister, A., Boiadjiev, S. E., and Lightner, D. A. (1999) Dissociation constants of carboxylic acids by ^{13}C NMR in DMSO/water, *Tetrahedron Lett. 40*, 8515−8518.
23. Mukerjee, P., and Ostrow, J. D. (1998) Effects of added dimethyl sulfoxide on p*Ka* values of uncharged organic acids and pH values of aqueous buffers, *Tetrahedron Lett. 39*, 423−426.
24. Ostrow, J. D., Pascolo, L., Shapiro, S. M., and Tiribelli, C. (2003) New concepts in bilirubin encephalopathy, *Eur. J. Clin. Invest. 33*, 988−997.
25. Ostrow, J. D., and Tiribelli, C. (2001) New concepts in bilirubin neurotoxicity and the need for studies at clinically relevant bilirubin concentrations, *J. Hepatol. 34*, 467−470.
26. Brito, M. A., Brondino, C. D., Moura, J. J., and Brites, D. (2001) Effects of bilirubin molecular species on membrane dynamic properties of human erythrocyte membranes: a spin label electron paramagnetic resonance spectroscopy study, *Arch. Biochem. Biophys. 387*, 57−65.
27. Fontich, M., Fors, P., Sese, M. L., and Trull, F. R. (1994) Polymer bound pyrrole compounds. VIII. Water-soluble pyrrole pigments carrying polyether side chains, *Eur. Polym. J. 30*, 1143−1149.
28. McDonagh, A. F., and Assisi, F. (1972) The ready isomerization of bilirubin IXα in aqueous solution, *Biochem. J. 129*, 797−800.
29. Dust, J. M., Fang, Z. H., and Harris, J. M. (1990) Proton NMR characterization of poly(ethylene glycols) and derivatives, *Macromolecules 23*, 3742−3746.
30. Harris, J. M., and Herati, R. S. (1991) Synthesis of polyethylene glycol thiol, *Polymer Prepr. 32*, 154−155.
31. Monti, D., and Manitto, P. (1981) A simple procedure for preparing bilirubin XIIIα, *Synth. Commun. 11*, 811−815.
32. Zalipsky, S., Gilon, C., and Zilkha, A. (1983) Attachment of drugs to polyethylene glycols, *Eur. Polym. J. 19*, 1177−1183.
33. Lewis, G. N., and Randall, M. (1923) *Thermodynamics*, McGraw-Hill, New York.
34. Huggins, M. T., and Lightner, D. A. (2000) Semirubin. A novel dipyrrinone strapped by intramolecular hydrogen bonds, *J. Org. Chem. 65*, 6001−6008.
35. Fujita, H. (1962) *Mathematical theory of sedimentation analysis*, Academic Press, New York.
36. Lamm, O. (1929) Die Differentialgleichung der Ultrazentrifugierung, *Ark. Mat. Astronom. Fys. 21B*, 1−6.
37. Behlke, J., and Ristau, O. (1997) Molecular mass determination by sedimentation velocity experiments and direct fitting of the concentration profiles, *Biophys. J. 72*, 428−434.
38. Tanford, C. (1961) in *Physical Chemistry of Macromolecules*, J. Wiley & Sons, New York.
39. Bull, H. B. (1943) *Physical Biochemistry*, p 289, J. Wiley & Sons, New York.
40. Bauer, N., and Lewin, S. Z. (1972) in *Physical Methods of Chemistry* (Weissberger, A., and Rossiter, B. W., Eds.) Part IV, p 70, J. Wiley & Sons, New York. See also Sillen, L. G., Lange, P. W., and Gabrielson, C. O. (1952) *Problems in Physical Chemistry*, p 49, Prentice-Hall, New York.
41. McDonagh, A. F., and Assisi, F. (1972) Direct evidence for the acid-catalyzed isomeric scrambling of bilirubin IXα, *J. Chem. Soc., Chem. Commun.* 117−119.

42. Brower, J. O., Lightner, D. A., and McDonagh, A. F. (2001) Aromatic congeners of bilirubin: synthesis, stereochemistry, glucuronidation and hepatic transport, *Tetrahedron 57*, 7813−7827.
43. Cifuentes, A., Bernal, J. L., and Diez-Masa, J. C. (1997) Determination of critical micelle concentration values using capillary electrophoresis instrumentation, *Anal. Chem. 69*, 4271−4274.
44. *CRC Handbook of Chemistry and Physics*, 64th ed., p D-167, CRC Press, Boca Raton, FL.
45. Falk, H. (1989) *The Chemistry of Linear Oligopyrroles and Bile Pigments*, Springer-Verlag, Wien.
46. Bonnett, R., Davies, J. E., and Hursthouse, M. B. (1976) Structure of bilirubin, *Nature 262*, 326−328.
47. Person, R. V., Peterson, B. R., and Lightner, D. A. (1994) Bilirubin conformational analysis and circular dichroism, *J. Am. Chem. Soc. 116*, 42−59.
48. Bonnett, R., Davies, J. E., Hursthouse, M. B., and Sheldrick, G. M. (1978) The structure of bilirubin, *Proc. R. Soc. London, Ser. B 202*, 249−268.
49. Le Bas, G., Allegret, A., Mauguen, Y., De Rango, C., and Bailly, M. (1980) The structure of triclinic bilirubin chloroform-methanol solvate, *Acta Crystallogr., Sect. B 36*, 3007−3011.
50. Mugnoli, A., Manitto, P., and Monti, D. (1983) Structure of bilirubin IXα (isopropylammonium salt) chloroform solvate, $C_{33}H_{34}N_4O_6^{2-}.2C_3H_{10}N^+.2CHCl_3$, *Acta Crystallogr., Sect. C 39*, 1287−1291.
51. Ostrow, J. D., and Celic, L. (1984) Bilirubin chemistry, ionization and solubilization by bile salts, *Hepatology 4*, 38S−45S.
52. Dörner, T., Knipp, B., and Lightner, D. A. (1997) Heteronuclear NOE analysis of bilirubin solution conformation and intramolecular hydrogen bonding, *Tetrahedron 53*, 2697−2716.
53. Kaplan, D., and Navon, G. (1982) Studies of the conformation of bilirubin and its dimethyl ester in dimethyl sulfoxide solutions by nuclear magnetic resonance, *Biochem. J. 201*, 605−613.
54. Manitto, P., and Monti, D. (1976) Free-energy barrier of conformational inversion in bilirubin, *J. Chem. Soc., Chem. Commun.* 122−123.
55. Overbeek, T. T. G., Vink, C. L. J., and Deenstra, H. (1955) The solubility of bilirubin, *Recl. Trav. Chim. Pays-Bas. 74*, 81−84.
56. Gray, C. H., Kulczycka, A., and Nicholson, D. C. (1961) The chemistry of the bile pigments. Part IV. Spectrophotometric titration of the bile pigments, *J. Chem. Soc.* 2276−2285.
57. Lucassen, J. (1961) The diazo reaction of bilirubin and bilirubin diglucuronide, Doctoral dissertation, University of Utrecht, Utrecht, The Netherlands.
58. Krasner, J., and Yaffe, S. J. (1973) The automatic titration of bilirubin, *Biochem. Med. 7*, 128−134.
59. Irollo, R., Casteran, M., Dang Vu, B., and Yonger, J. (1979) Étude de la liaison bilirubine-albumin I − Étude in vitro par une méthode de partage de la bilirubine entre une solution aqueuse et un solvant organique non miscible à l'eau, *Ann. Biol. Clin. 37*, 331−342.
60. Hahm, J. S., Ostrow, J. D., Mukerjee, P., and Webster, C. C. (1986) Solubility and p*K*'a of unconjugated bilirubin in aqueous buffer and bile salt solutions, determined by isoextraction from chloroform, *Hepatology 6*, 1185 (Abstract).
61. Westheimer, F. H., and Benfey, O. T. (1956) The quantitative evaluation of the effect of hydrogen bonding on the strength of dibasic acids, *J. Am. Chem. Soc. 78*, 5309−5311.
62. Kurtin, W. E., Enz, J., Dunsmoor, C., Evans, N., and Lightner, D. A. (2000) Acid dissociation constants of bilirubin and related carboxylic acid compounds in bile salt solutions, *Arch. Biochem. Biophys. 381*, 83−91.
63. Mukerjee, P., Ostrow, J. D., and Tiribelli, C. (2002) Low solubility of unconjugated bilirubin in dimethylsulfoxide-water systems: implications for pK_a determinations, *BMC Biochem. 3*, 17.
64. Ostrow, J. D. (1995) Bilitec to quantitate duodenogastric reflux: is it valid? *Gastroenterology 108*, 1332−1334.
65. Zucker, S. D., Goessling, W., Bootle, E. J., and Sterritt, C. (2001) Localization of bilirubin in phospholipid bilayers by parallax analysis of fluorescence quenching, *J. Lipid Res. 42*, 1377−1388.
66. Chung, T. W., Cho, K. Y., Nah, J. W., Akaike, T., and Cho, C. S. (2002) Chiral recognition of bilirubin by polymeric nanoparticles, *Langmuir 18*, 6462−6464.
67. Parks, J. S., Cistola, D. P., Small, D. M., and Hamilton, J. A. (1983) Interactions of the carboxyl group of oleic acid with bovine serum albumin: a ^{13}C NMR study, *J. Biol. Chem. 258*, 9262−9269.
68. Cistola, D. P. (1985) Physicochemical studies of fatty acids in model biological systems. Ph.D. dissertation, Boston University; *Chem. Abstr. 105*, 148490, 245 pp.
69. Hamilton, J. A. (1994) in *Carbon-13 NMR Spectroscopy of Biological Systems* (Beckmann, N., Ed.) pp 117−157, Academic Press, New York.
70. Kanicky, J. R., and Shah, D. O. (2002) Effect of degree, type, and position of unsaturation on the pK_a of long-chain fatty acids, *J. Colloid Interface Sci. 256*, 201−207.
71. Kanicky, J. R., and Shah, D. O. (2003) Effect of premicellar aggregation on the pK_a of fatty acid soap solutions, *Langmuir 19*, 2034−2038.
72. Small, D. M., Cabral, D. J., Cistola, D. P., Parks, J. S., and Hamilton, J. A. (1984) The ionization behavior of fatty acids and bile acids in micelles and membranes, *Hepatology 4*, 77S−79S.
73. Ptak, M., Egret-Charlier, M., Sanson, A., and Bouloussa, O. (1980) A NMR study of the ionization of fatty acids, fatty amines and N-acylamino acids incorporated in phosphatidylcholine vesicles, *Biochim. Biophys. Acta 600*, 387−397.
74. Kepczynski, M., and Ehrenberg, B. (2002) Interaction of dicarboxylic metalloporphyrins with liposomes. The effect of pH on membrane binding revisited, *Photochem. Photobiol. 76*, 486−492 and references therein.
75. Brodersen, R. (1982) in *Bilirubin. Vol. I Chemistry* (Heirwegh, K. P. M., and Brown, S. B., Eds.) pp 75−123, CRC Press, Inc., Boca Raton, FL.
76. Brodersen, R., and Theilgaard, J. (1969) Bilirubin colloid formation in neutral aqueous solution, *Scand. J. Clin. Lab. Invest. 24*, 395−398.
77. Brodersen, R. (1966) Dimerization of bilirubin anion in aqueous solution, *Acta Chem. Scand. 20*, 2895−2896.
78. Carey, M. C., and Koretsky, A. P. (1979) Self-association of unconjugated bilirubin-IX alpha in aqueous solution at pH 10.0 and physical-chemical interactions with bile salt monomers and micelles, *Biochem. J. 179*, 675−689.
79. Carey, M. C., and Spivak, W. (1986) in *Bile Pigments and Jaundice* (Ostrow, J. D., Ed.) pp 81−132, Marcel Dekker, Inc., New York.
80. Mammen, M., Simanek, E. E., and Whitesides, G. M. (1996) Predicting the relative stabilities of multiparticle hydrogen-bonded aggregates based on the number of hydrogen bonds and the number of particles and measuring these stabilities with titrations using dimethyl sulfoxide, *J. Am. Chem. Soc. 118*, 12614−12623.
81. Patra, S. K., Mandal, A. K., and Pal, M. K. (1999) State of aggregation of bilirubin in aqueous solution: principal component analysis approach, *J. Photochem. Photobiol. A: Chem. 122*, 23−31.
82. Persson, B. O., Drakenberg, T., and Lindman, B. (1979) Carbon-13 NMR of micellar solutions. Micellar aggregation number from the concentration dependence of the carbon-13 chemical shifts, *J. Phys. Chem. 83*, 3011−3015.
83. Cohen, A. N., and Ostrow, J. D. (1980) New concepts in phototherapy: photoisomerization of bilirubin IX alpha and potential toxic effects of light, *Pediatrics 65*, 740−750.
84. Ostrow, J. D., and Cohen, A. N. (1981) New concepts in phototherapy: photoisomerization of bilirubin IXα and potential toxic effects of light, *Pediatrics 67*, 930−931.
85. Tiribelli, C., and Ostrow, J. D. (1993) New concepts in bilirubin chemistry, transport and metabolism: report of the Second International Bilirubin Workshop, April 9−11, 1992, Trieste, Italy, *Hepatology 17*, 715−736.
86. Onoda, A., Yamada, Y., Takeda, J., Nakayama, Y., Okamura, T., Doi, M., Yamamoto, H., and Ueyama, N. (2004) Stabilization of carboxylate anion with a NH···O hydrogen bond: facilitation of the deprotonation of carboxylic acid by the neighboring amide NH groups, *Bull. Chem. Soc. Jpn. 77*, 321−329.
87. Walker, J. (1892) The dissociation constants of organic acids, *J. Chem. Soc. 61*, 696−716.
88. Rebek, J., Jr., Duff, R. J., Gordon, W. E., and Parris, K. (1986) Convergent functional groups provide a measure of stereoelectronic effects at carboxyl oxygen, *J. Am. Chem. Soc. 108*, 6068−6069.
89. Newcomb, M., Moore, S. S., and Cram, D. J. (1977) Host−guest complexation. 5. Convergent functional groups in macrocyclic polyethers, *J. Am. Chem. Soc. 99*, 6405−6410.
90. Gennari, C., Molinari, F., Bartoletti, M., and Potenza, D. (1992) A new macrocyclic diacid with balanced conformational flexibility and preorganization, *Gazz. Chim. Ital. 122*, 279−282.

91. Bell, T. W., Cheng, P. G., Newcomb, M., and Cram, D. J. (1982) Host−guest complexation. 24. Synthesis of multiheteromacrocycles containing intramolecularly interacting units or new steric barriers, *J. Am. Chem. Soc. 104*, 5185−5188.
92. Eberson, L., and Wadsö, I. (1963) Intramolecular hydrogen bonding as a factor in determining the K_1/K_2 ratios of dicarboxylic acids, *Acta Chem. Scand. 17*, 1552−1562.
93. McDonagh, A. F. (1979) in *The Porphyrins* (Dolphin, D., Ed.) Vol. VI, pp 293−491, Academic Press, New York.
94. Gawronski, J. K., Polonski, T., and Lightner, D. A. (1990) Sulfoxides as chiral complexation agents. Conformational enantiomer resolution and induced circular dichroism of bilirubins, *Tetrahedron 46*, 8053−66.
95. Puzicha, G., Pu, Y. M., and Lightner, D. A. (1991) Allosteric regulation of conformational enantiomerism. Bilirubin, *J. Am. Chem. Soc. 113*, 3583−3592.
96. Pu, Y. M., and Lightner, D. A. (1991) On the conformation of bilirubin dianion, *Tetrahedron 47*, 6163−6170.
97. Boiadjiev, S. E., Person, R. V., Puzicha, G., Knobler, C., Maverick, E., Trueblood, K. N., and Lightner, D. A. (1992) Absolute configuration of bilirubin conformational enantiomers, *J. Am. Chem. Soc. 114*, 10123−10133.
98. Weisiger, R. A., Ostrow, J. D., Koehler, R. K., Webster, C. C., Mukerjee, P., Pascolo, L., and Tiribelli, C. (2001) Affinity of human serum albumin for bilirubin varies with albumin concentration and buffer composition: results of a novel ultrafiltration method, *J. Biol. Chem. 276*, 29953−29960.
99. Briz, O., Serrano, M. A., MacIas, R. I., Gonzalez-Gallego, J., and Marin, J. J. (2003) Role of organic anion-transporting polypeptides, OATP-A, OATP−C and OATP-8, in the human placenta-maternal liver tandem excretory pathway for foetal bilirubin, *Biochem. J. 371*, 897−905.
100. Ostrow, J. D., Pascolo, L., and Tiribelli, C. (2002) Mechanisms of bilirubin neurotoxicity, *Hepatology 35*, 1277−1280.
101. Ostrow, J. D., Pascolo, L., and Tiribelli, C. (2003) Reassessment of the unbound concentrations of unconjugated bilirubin in relation to neurotoxicity in vitro, *Pediatr. Res. 54*, 98−104.
102. Ostrow, J. D., Pascolo, L., and Tiribelli, C. (2003) *Pediatr. Res. 54*, 926.

BI0481491